THESIS FOR THE DEGREE OF DOCTOR OF PHILOSOPHY

Precipitation of Kraft Lignin

Yield and Equilibrium

WEIZHEN ZHU

Forest Products and Chemical Engineering
Department of Chemistry and Chemical Engineering

CHALMERS UNIVERSITY OF TECHNOLOGY

Gothenburg, Sweden 2015

Precipitation of Kraft Lignin

Yield and Equilibrium

WEIZHEN ZHU

Department of Chemistry and Chemical Engineering

Chalmers University of Technology

SE-412 96 Gothenburg

Sweden

Telephone + 46 (0)31-772 1000

Cover:

[Left: A beaker of softwood black liquor and precipitated softwood kraft lignin. Right: SEM image of precipitated softwood kraft lignin (magn. 725 x)]

Precipitation of Kraft Lignin

Yield and Equilibrium

WEIZHEN ZHU

Forest Products and Chemical Engineering

Department of Chemistry and Chemical Engineering

Chalmers University of Technology

ABSTRACT

Kraft pulping is the dominant pulping process used in the world today. The material efficiency in modern kraft pulp mills is, however, only 40−55% and the final product consists mainly of cellulose. Recently, a novel process called "LignoBoost" has been introduced to separate lignin from kraft black liquor. The separated lignin can be utilized either as a solid fuel or as a raw material for the production of carbon fibres or chemicals. It makes it possible for a traditional pulp mill to become a combined biorefinery. There are four major steps in the LignoBoost process: precipitation of lignin, filtration of lignin, re-dispersion of the lignin suspension and, finally, washing of lignin. The filtration and washing steps have been investigated extensively already, so it is of interest to gain more knowledge regarding the precipitation of lignin.

Two kraft black liquors were used in this work: a mixed hardwood/softwood black liquor and a softwood black liquor. Cross-flow filtration was used to fractionate lignin with a different molecular weight from the softwood black liquor. The precipitation of lignin was performed by acidifying the black liquor at various process conditions, namely pH, temperature and ionic strength of the black liquor. The influences exerted by these parameters on the precipitation yield of lignin were investigated. The molecular properties (average molecular weight and functional groups) of precipitated lignin, together with a carbohydrate analysis of the black liquor and precipitated lignin, were determined. Finally, the dissociation degree of the phenolic groups on the lignin molecules was estimated using the Poisson-Boltzmann cell model.

The results show that the precipitation yield of lignin increases with decreasing pH and temperature and/or with increasing ionic strength of the black liquor. There is an increasing amount of lignin with a lower molecular weight that is precipitated at a higher yield. Within the same precipitation conditions, the lignin fraction with the highest molecular weight tends to have the highest yield. According to NMR analysis of lignin, the content of methoxyl groups decreases for softwood lignin but increases for mixed hardwood/softwood lignin at a higher yield, whereas the content of phenolic groups increases at a higher yield for both types of lignin. The content of carbohydrates decreases with increasing yield. In a highly electrolyte solution (such as black liquor), the dissociation degree of the phenolic groups on the lignin molecules is related to the alkalinity and temperature of the precipitation conditions, but less so to an increase in the ionic strength or the molecular weight of the lignin.

Keywords: LignoBoost process, lignin precipitation, black liquor, Poisson-Boltzmann cell model, molecular weight of lignin, ^{1}H and ^{13}C NMR spectra of lignin.

List of publications

This thesis is based on the studies presented in following papers:

I.   **Investigation and characterization of lignin precipitation in the LignoBoost process**

Weizhen Zhu, Gunnar Westman and Hans Theliander

Journal of Wood Chemistry and Technology 34(2), 77-97, 2013

II.   **The molecular properties and carbohydrate content of lignins precipitated from black liquor**

Weizhen Zhu, Gunnar Westman and Hans Theliander

Holzforschung 69 (2), 143-152, 2015

III.   **Precipitation of lignin from softwood black liquor: an investigation of the equilibrium and molecular properties of lignin**

Weizhen Zhu and Hans Theliander

BioResources 10 (1), 1696-1714, 2015

IV.   **Lignin separation from kraft black liquor by combined ultrafiltration and precipitation: a study of lignin solubility with different molecular properties**

Weizhen Zhu, Gunnar Westman and Hans Theliander

Submitted

V.   **Theoretical estimation of the dissociation degree of phenolic groups on kraft lignin from the LignoBoost process**

Weizhen Zhu, Tor Sewring, Maria Sedin and Hans Theliander

In manuscript, to be submitted

Results relating to this work have also been presented at the following conference:

Equilibrium of lignin precipitation

Weizhen Zhu and Hans Theliander

(Poster presentation)
In: Conference proceedings. *16th International Symposium on Wood, Fibre and Pulping Chemistry*, pp 195-199, Tianjin, China, June 8-10, 2011

Contribution report

The author of this thesis has made the following contributions to the papers:

I.   First author. Active in planning the experimental outline, performing the experimental work, interpreting the results and writing the paper under the supervision of Prof. Gunnar Westman and Prof. Hans Theliander.

II.   First author. Active in planning the experimental outline, performing the experimental work and interpreting the results and writing the paper under the supervision of Prof. Gunnar Westman and Prof. Hans Theliander.

III.   First author. Active in planning the experimental outline, performing the experimental work and interpreting the results and writing the paper under the supervision of Prof. Hans Theliander.

IV.   First author. Active in planning the experimental outline, performing the experimental work and interpreting the results and writing the paper under the supervision of Prof. Gunnar Westman and Prof. Hans Theliander.

V.   First author. Active in planning the experimental outline, performing the experimental work and writing the majority of the paper. Active in the theory part of the paper and made an equal and joint effort in the results and discussion parts under the supervision of Dr. Maria Sedin and Prof. Hans Theliander.

行到水窮處，坐看雲起時。

－《終南別業》王維（公元 699-759）

Where a mountain stream ends, there starts a journey of rain.

My Retreat at Mount Zhongnan　Wang Wei (C.E. 699-759)

Contents

x

1. INTRODUCTION AND OBJECTIVES

1.1 Introduction

The forest industry forms a cornerstone of Sweden's economy and is thereby one of its most important industrial sectors. It accounts for approximately 3% of the Swedish gross domestic product (GDP) (Skogsindustrierna, 2010) and 9-12% of the total employment, sales and added-value products within Swedish industry (Skogsindustrierna, 2014). The forest industry is heavily export orientated and contributes to a significant share of the country's trade balance. Sweden is the third largest combined exporter of pulp, paper and sawn wood products in the world (Skogsindustrierna, 2014), of which the pulp and paper industry in particular is the second largest in Europe. It may be mentioned that in excess of 90% of the pulp and paper produced in Sweden is exported to other countries which, in 2013, was valued at 120 billion SEK (Skogsindustrierna, 2014).

The predominant pulping process employed in Sweden is the kraft process. In 2013, the amount of kraft pulp produced was approx. 8 million metric tons, comprising around 70% of the total amount of pulp produced (Skogsindustrierna, 2014). Moreover, the tendency during the past few years has been a decrease in the percentage of mechanical and semi-chemical pulp in the total pulp production (Skogsindustrierna, 2014).

A schematic diagram of the kraft pulping process is illustrated in Fig. 1.1. Firstly, the wood chips are treated with steam and impregnated with cooking liquor. The impregnated wood chips are digested in either a batch or a continuous digester at an elevated temperature (150–170°C) (Gullichsen, 1999). The primary aims of cooking are to remove lignin from the wood chips and liberate the fibres from each other. The active chemicals in the cooking liquor are NaOH and Na_2S, in which the corresponding OH^- and HS^- ions are the active reactants. The main reaction during kraft cooking is delignification, whereby the linkages of the lignin network are degraded and more free phenolic groups of lignin are formed. The degraded lignin fragments are more hydrophilic in the alkaline cooking liquor due to the increasing amount of free phenolic groups (Gellerstedt, 2009). The solubility of lignin is therefore increased and the lignin dissolves in the cooking liquor. Some of the cellulose and hemicelluloses are also degraded and dissolved during cooking, however, which decreases the cooking yield. After cooking, the solution that then consists of dissolved lignin, other organic materials (*e.g.* polysaccharides, carboxylic acids and extractives), inorganic compounds and spent cooking chemicals is known as "black liquor" (BL) and is separated from the pulp in the "brown-stock washing" department. The washed pulp can either be used in various unbleached packaging products or transferred to the bleaching plant to produce bleached pulp. The BL is then fed to an evaporation plant where most of the water is evaporated and the total dry solid content (TDS) is increased from approx. 15% to 70–80% (Frederick, 1997). The BL, which contains most of the dissolved organic compounds, is then incinerated in a recovery boiler where some of the cooking chemicals are recovered and steam is generated. The steam is used for heating and for producing electric power.
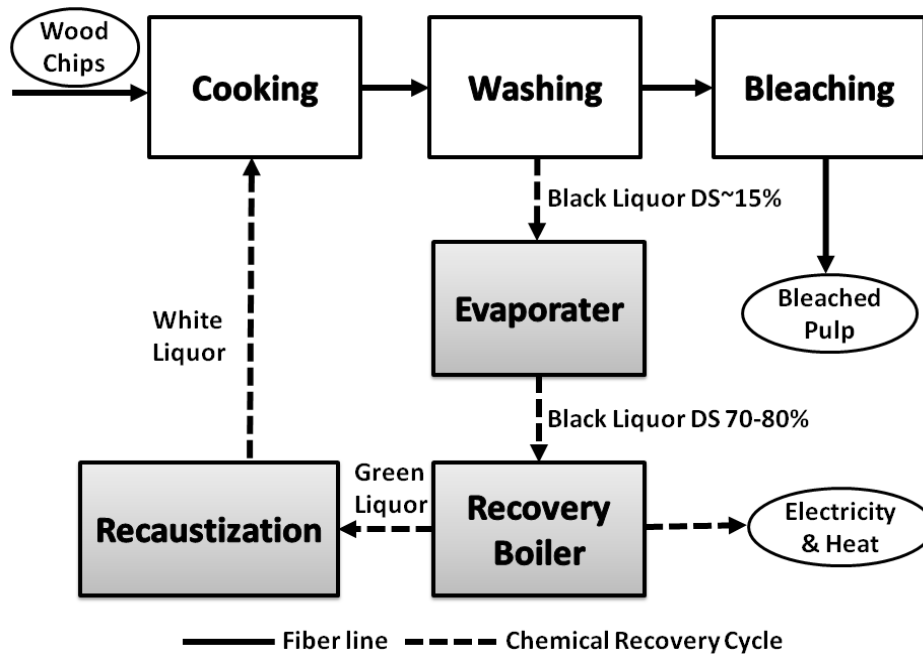
Figure 1.1 Schematic diagram of the kraft pulping process.

The kraft process has a yield of only approx. 40–55%; so far, cellulose is the only main component of wood that has been utilized efficiently in the production of materials. Vast quantities of kraft lignin (estimated at 5.5×10^7 metric tons per year) are produced worldwide (Gellerstedt *et al.*, 2012). However, more than 99% of it is incinerated in the chemical recovery boiler and is not recovered for other industrial applications (Pye, 2008). The separation of lignin makes it possible to transform the dissolved lignin into a solid fuel that can be used internally in the pulp mill either as a replacement for the fuel oil consumed in the lime kiln or sold to other industries. Furthermore, the separated lignin can be used as a raw material for other value-added products, *e.g.* carbon fibres (Sudo and Shimizu, 1992, Gellerstedt *et al.*, 2010) and chemicals (such as phenols and benzene) which require lignin with a high level of purity: Table 1.1 shows some of the potential applications of lignin. Thus, the separation of lignin from BL creates new opportunities for converting a modern kraft pulp mill into a biorefinery, thereby improving the total material yield of the mill. The pulp and paper industry can therefore remain competitive by creating new revenues and diversifying its products and markets.

In some cases, it is of great benefit to withdraw a certain amount of lignin from BL since lignin is the greatest contributor to the heating value of BL: the heat load of the recovery boiler will be decreased if a certain amount of lignin is removed from the BL. This would be beneficial in pulp mills where the capacity of the recovery boiler limits the overall production rate of pulp (Wallmo *et al.*, 2009c).

Table 1.1 Potential applications of lignin (Bozell *et al.*, 2007, Higson, 2011).

Applications	Products
Syngas	Methanol, DME, Ethanol, Mixed alcohols, Fisher-Tropsch liquids, C_1-C_7 gases
Hydrocarbons	Benzene, Toluene, Xylene, Cyclohexane, Styrene, Biphenyls
Phenols	Phenol, Substituted phenols, Catechols, Cresols, Resorcinols eugenol, Syringols, Coniferols, Guaiacols
Oxidized chemicals	Vanillin, Vanillic acid, DMSO, Aromatic acids, Aliphatic acids, Syrigaldehyde, Aldehydes, Quinines, Cyclohexanol
Macromolecules	Carbon fibres, Polymer extenders, Substituted lignins, Thermoset resins, Composites, Adhesives, Binders, Pharmaceuticals, Polyols

1.2 Objectives

The primary objective of the work in this thesis was to investigate the fundamentals of lignin precipitation in BL and, more specifically, the yield of the lignin precipitation. Two types of BL, obtained from different wood origins, were used: one softwood kraft BL and one mixed hardwood/softwood kraft BL. The influences of some important process parameters, namely pH, temperature and ionic strength of the BL on the yield of lignin precipitation were investigated. The influence of some molecular properties (*e.g.* molecular weight and functional groups) of lignin on its precipitation was also studied. Also, a combination of the ultrafiltration of BL and the precipitation of lignin was evaluated, and the precipitation behaviour of lignin molecules with different molecular weights (MW) was investigated. A theoretical model describing the dissociation of phenolic groups on lignin molecules was proposed and then used to investigate the relationship between the precipitation yield and the dissociation degree of the phenolic groups.

1.3 Outline

Chapter 2 provides background information regarding lignin and BL. A brief introduction of lignin chemistry during kraft cooking and a description of the black liquor system from a chemical perspective are included. Several lignin separation technologies, particularly the "LignoBoost" process, are also presented. The mechanism of lignin precipitation and the estimation of the dissociation degree of phenolic groups of lignin using the Poisson-Boltzmann cell model are described in Chapter 3. Chapter 4 contains the experimental work pertaining to lignin precipitation and the fractionation of lignin by membrane filtration of black liquor; the analytical characterisation of black liquor filtrate and precipitated lignin are also given. The results of the precipitation yields (the influence of pH, temperature, ionic strength addition, MW and functional groups of kraft lignin) and the analysis of carbohydrates in BL and precipitated lignin, together with a theoretical study of the dissociation of phenolic groups on lignin molecules, are presented in Chapter 5. The main findings are summarized in Chapter 6 and potential future work is proposed in Chapter 7.

2. LIGNIN AND BLACK LIQUOR

2.1 Lignin

2.1.1 Native lignin

The three main components of lignocellulosic biomass are cellulose, hemicelluloses (mostly (galacto)glucomannan (GGM) and xylan) and lignin. After cellulose, lignin is not only the second most abundant polymeric organic substance on the planet but also the most abundant aromatic renewable material (Gellerstedt and Henriksson, 2008). It is a three-dimensional, heterogeneous polymer that "adheres" the fibres in the middle lamella and the fibrils in the cell wall together. The unique mechanical properties of wood are derived partially from lignin. Lignin also provides woody biomass with stiffness, hydrophobicity and resistance to bacterial degradation (Henriksson *et al.*, 2009).

The amount of lignin present in softwood is 26–32% (spruce approx. 27%) and in hardwood 20–26% (birch approx. 22%). Around 70% of softwood (spruce) lignin and 60% of hardwood (birch) lignin is found in the secondary cell wall. The remaining lignin in softwood is present between the fibres, *i.e.* in the middle lamella and cell corners (Sjöström, 1993).

The sub-units comprising lignin are phenylpropane units, as shown in Fig. 2.1. The guaiacyl propane unit (G-type) is the most abundant in native softwood lignin, while hardwood lignin contains approximately equal amounts of G-type and syringyl propane units (S-type). The phenylpropane units are joined together with both Carbon-Oxygen-Carbon (C-O-C, ether) and Carbon-Carbon (C-C) linkages: the ether bond dominates, accounting for approx. two thirds of the total linkages (Sjöström, 1993). The types of linkage and their approximate proportion are shown in Table 2.1.
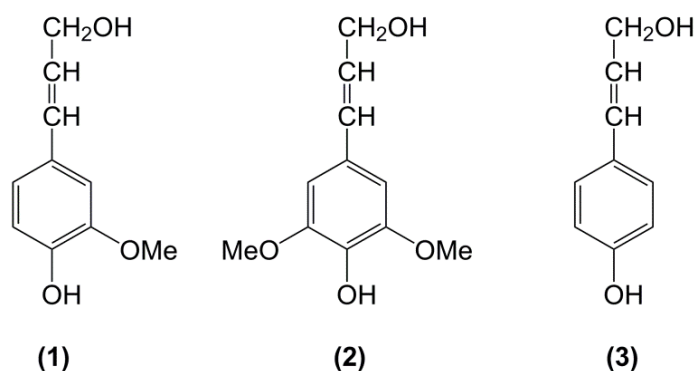

Figure 2.1 The building units in lignin: (1) guaiacyl propane, (2) syringyl propane, (3) *p*-hydroxyphenyl propane (Adler, 1977).

The functional groups in lignin (see Fig. 2.2), such as phenolic and methoxyl (OMe) groups, affect the reactivity of lignin strongly. These groups are listed in Table 2.2 along with their approximate quantities.

Table 2.1 The types of linkages connecting the phenylpropane units in lignin and their approximate proportions (Sjöström, 1993).

Linkage type	Dimer structure	Percentage of the total linkages (%)	
		Softwood lignin	Hardwood lignin
β-O-4	Arylglycerol-β-aryl ether	50	60
α-O-4	Noncyclic benzyl aryl ether	2–8	7
β-5	Phenylcoumaran	9–12	6
5-5	Biphenyl	10–11	5
4-O-5	Diaryl ether	4	7
β-1	1,2-Diaryl propane	7	7
β-β	Linked through side chains	2	3
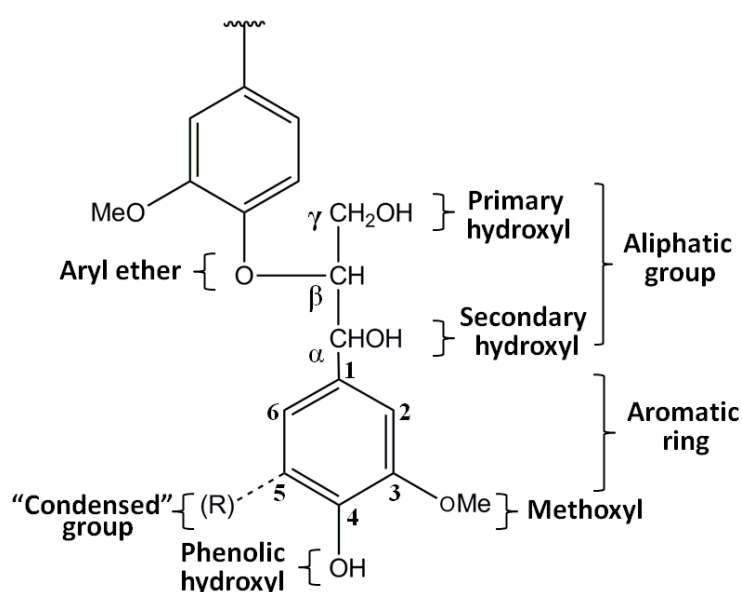
Figure 2.2 The functional groups in lignin. Adapted from Donald (2010).

Table 2.2 The functional groups in lignin per 100 C_9 units (Sjöström, 1993).

Functional group	Softwood lignin	Hardwood lignin
Methoxyl	92–97	139–158
Phenolic	15–30	10–15
Benzyl alcohol	30–40	40–50
Carbonyl	10–15	

The possible linkages that can be expected between the lignin sub-units are illustrated in Fig. 2.3, which shows a random, cross-linked, amorphous network of softwood lignin. Hardwood lignin differs mainly in the content of the methoxyl group. It is important to emphasize that this proposed model does not depict the actual structure of lignin: it serves, instead, as a tool to visualize the linkages and functional groups in lignin.
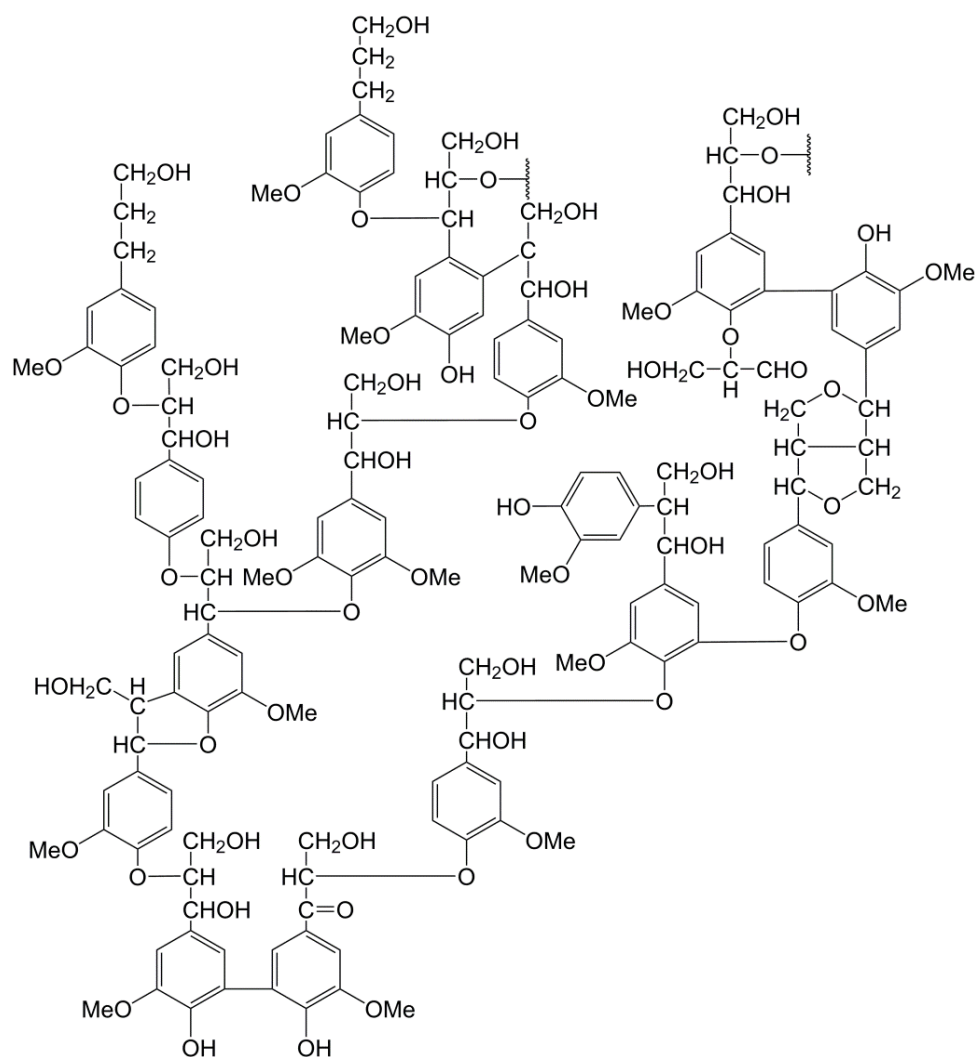
Figure 2.3 A representation of the hypothetical linkages and functional groups of native softwood lignin. Adapted from Adler (1977).

2.1.2 Lignin-carbohydrate complex

Another major component of the cell wall of wood is hemicellulose, which is a group of branched heteropolysaccharides. Chemical covalent bonds have been reported between lignin and hemicelluloses (Merewether, 1957, Eriksson *et al.*, 1980); these covalently-bonded complexes are often given the term "lignin-carbohydrate complex" (LCC). So far, several kinds of lignin-carbohydrates bonds have been proposed that include 1) benzyl ether, 2) benzyl ester, 3) phenyl glycoside and 4) acetal types (Watanabe, 2003). The principal hemicellulose in softwood is GGM and accounts for approx. 20% of the dry material, whilst the main hemicellulose in hardwood is xylan and varies in content within the limits of 15–30% of the dry wood.

During kraft pulping, the network between the lignin and hemicellulose molecules disintegrates; smaller LCC fragments are formed which, in turn, dissolve in the BL (Gellerstedt and Lindfors, 1984). Tamminen *et al.* (1995) reported that LCC was present in BL, and that it was likely that xylan was cross-linked to lignin molecule by the arabinose

substituent. Compared with xylan, GGM is degraded more extensively as the results of peeling and alkaline hydrolysis reactions during the kraft pulping process (Sjöström, 1993). On the other hand, it has been suggested that xylan-lignin LCC is more exposed under alkaline conditions due to the relatively higher solubility of xylan, making it easier to break the xylan-lignin bond than the GGM-lignin bond (Lawoko *et al.*, 2004, Gellerstedt *et al.*, 2012).

2.1.3 Lignin reactions during kraft pulping

The predominant reaction that occurs in lignin during kraft pulping is the cleavage of its phenolic β-O-4 linkages, which results in the formation of new phenolic groups. This fragmentation causes a large decrease in the MW of lignin, and the degraded lignin becomes more hydrophilic as a result of the formation of the new phenolic groups (Gellerstedt, 2009). It also has been found that, during the initial delignification stage, the dissolved lignin is of low MW and contains higher amounts of phenolic groups whereas, towards the final delignification stage, larger lignin molecules containing increasing amounts of carbohydrates become dissolved (Gellerstedt and Lindfors, 1984). As a result, the high polydispersity of lignin molecules in black liquor (McNaughton *et al.*, 1967, Connors *et al.*, 1980) could be attributed to the variable degradation of soluble lignin during kraft cooking or, alternatively, to condensation reactions (Gierer, 1970, 1980, Chakar and Ragauskas, 2004, Gellerstedt, 2009).

During kraft cooking, the methyl-aryl ether bonds of the lignin sub-units are also cleaved off, to some extent, by the reaction of sulphur-containing nucleophilic species, *i.e.* hydrogen sulfide ion (HS^-) or methanethiolate ion (CH_3S^-) (Gellerstedt, 2009), see <u>Fig. 2.4</u>. The malodorous gases methanethiol (CH_3SH) and dimethyl sulphide (($CH_3)_2S$) are thereafter formed, causing malodorous problems for the immediate vicinity of kraft pulp mills (Gierer, 1980).
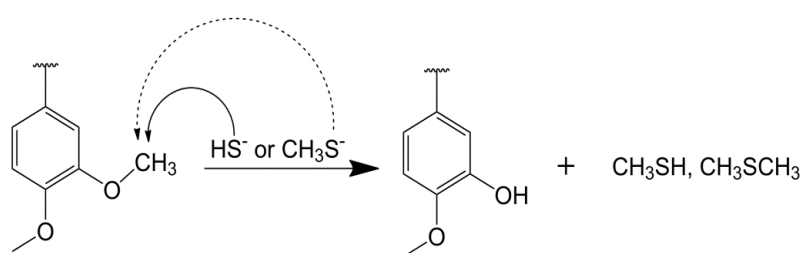

Figure 2.4 The cleavage reaction of the methyl-aryl ether bond of lignin in kraft pulping.

A hypothetical structure for kraft lignin is shown in <u>Fig. 2.5</u>. It can be seen that the degraded kraft lignin contains a large amount of free phenolic groups; some aliphatic hydroxyl and carboxyl groups are also formed during kraft cooking (Froass *et al.*, 1998). Moreover, it has been found that the average molecular weight of hardwood kraft lignin is lower than that of softwood kraft lignin (Goring, 1971). One reason for this might be that more β-O-4 linkages (Larsson and Miksche, 1971, Sjöström, 1993) are heavily degraded in hardwood lignin than in softwood lignin during the kraft pulping process. Another possible reason could be that

hardwood lignin (S-type) contains fewer C-C bonds between the S units (Labidi *et al.*, 2006) and thus has fewer reactive positions (C_5 positions) in the aromatic ring for condensation reactions (Mörck *et al.*, 1988).
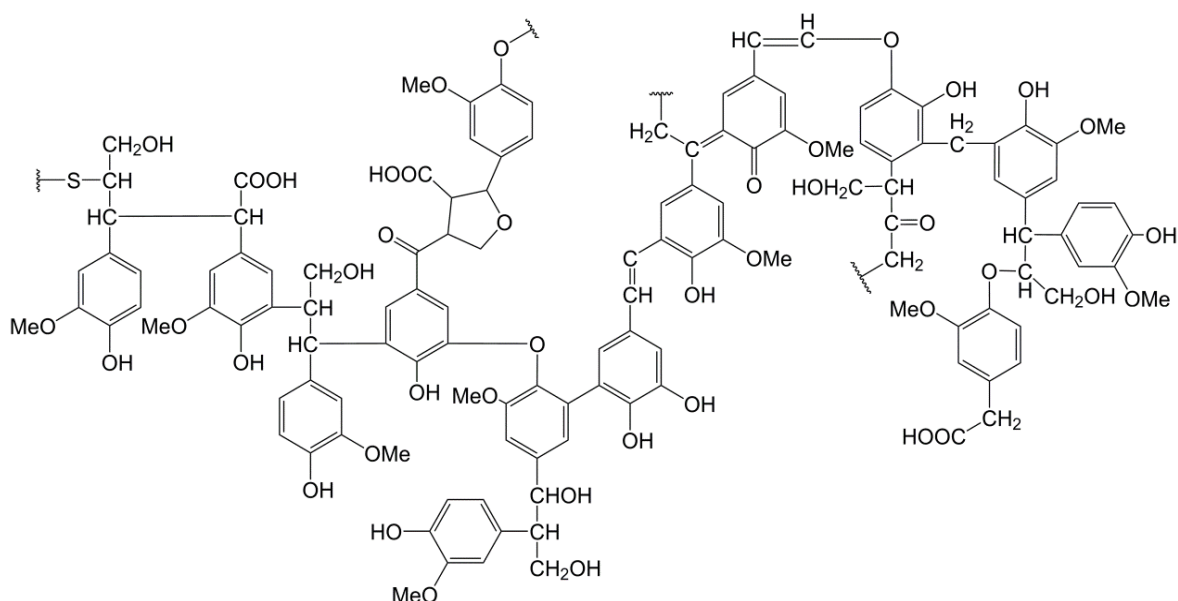

Figure 2.5. A hypothetical structure of softwood kraft lignin. Adapted from Marton (1971).

2.2 Black liquor

Black liquor is a process stream obtained from the digestion/washing stages in the chemical pulping process, as mentioned in Section 1.1. Typical softwood kraft black liquor has a pH of 12.5–13 and a TDS content after evaporation of up to 80% (Frederick, 1997). Lignin forms approximately 30–45% of the dry materials in BL while other chemical species, such as aliphatic carboxylic acids and inorganics, account for around 30% each in the dry materials (Frederick, 1997, Niemelä and Alén, 1999), see Table 2.3. The main inorganic ions in BL are cations such as Na^+ and K^+, and anions such as Cl^-, HS^-, SO_4^{2-}, SO_3^{2-}, $S_2O_3^{2-}$ and CO_3^{2-} (Niemelä and Alén, 1999). The organic materials in BL are almost completely dissolved due to the highly alkaline condition. The inorganic salts are dissociated into ionic species, so the ionic strength (IS) of BL is typically relatively high. The inorganic ions, together with the organic material, form a complex multicomponent system of electrolytes and macromolecules. The behaviour of lignin in BL, and its interactions with other compounds, are important for the properties of BL. From a chemical aspect, the lignin fragments can be regarded as being polydisperse macromolecules that contain functional groups, particularly phenolic groups. These groups are ionized into charged groups under highly alkaline conditions. The thermodynamic complexity of BL arises from the interactions between electrolytes and the charged surface of the polyelectrolytes (*e.g.* lignin macromolecules) together with the ion-ion interactions between the electrolytes.

It should be mentioned here that the proportions of organic and inorganic components in BL varies from mill to mill due to natural variations in the organic constituents of wood species and the cooking conditions that are unique to each mill. The properties of BL therefore also

vary depending on origin but also over with time within the same mill. Another important property of BL is that it is highly buffered. The buffer systems used are sulphide ($pK_a \approx 13$–13.5), carbonate ($pK_a \approx 10.2$) and phenolic ($pK_a \approx 9.4$–10.8) (The American Forest and Paper Association, 2003).

Table 2.3 Typical chemical compositions (% TDS) of softwood (pine) and hardwood (birch) kraft black liquors (Niemelä and Alén, 1999).

Chemical species	Pine	Birch
Alkali lignin	31	25
-High MW fraction (>500 Da)	28	22
-Low MW fraction (<500 Da)	3	3
Aliphatic carboxylic acids	29	31
-Acetic acid	4	8
-Formic acid	6	4
-Hydroxyl monoacids	16	17
-Hydroxyl diacids	3	2
Other organics	7	11
-Extractives	4	3
-Polysaccharides	2	7
-Miscellaneous	1	1
Inorganics	33	33
-Inorganic compounds	22	22
-Sodium	11	11

2.3 Separation of lignin from black liquor

2.3.1 The principle of lignin separation

Several techniques are available for the separation and purification of lignin from black liquor. These are based on either changing the solubility of lignin or fractionating lignin with a different MW, or a combination of both. The separation methods are based on three criteria being fulfilled: firstly, the lignin is isolated with a high yield; secondly, the isolated lignin is free from contaminants and, thirdly, the procedure is simple and easy to perform (Lin, 1992).

2.3.2 Methods used in lignin separation

2.3.2.1 Lignin precipitation

Extracting lignin from black liquor by means of acidification has been commercialized for a long period of time. In 1942, in the USA, the Westvaco Company (now MeadWestvaco Corporation) started to produce lignin from black liquor obtained from the kraft process, with an estimated annual production of 2.7×10^4 metric tons (Pye, 2008, Gellerstedt *et al.*, 2012). Kraft lignin was also sold by Borregaard LignoTech from 1994 to 2005. Recently, a lignin separation process called "LignoBoost", which will be discussed in <u>Section 2.3.3</u>, was

launched; a demonstration plant was established in Sweden to produce up to 8×10^3 metric tons per annum of lignin from black liquor (Innventia, 2007). The first commercial operation was started by Domtar in the USA in 2013, with an annual production of lignin of approx. 2.7 $\times 10^4$ metric tons (Finaldi, 2013). A second, full-scale LignoBoost plant has been scheduled for start-up by Stora Enso in Finland in early 2015, with an estimated annual production of kraft lignin of 5×10^4 metric tons (Valmet, 2013).

A number of studies related to lignin precipitation by acidification can be found in the literature. In 1872, a method in which carbon dioxide is injected into hot BL was patented (Tessie du Motay, 1872) with the aim of separating the "impurities" present in the liquor. The resulting, purer, BL can be recausticized and thereby reused. Later, in 1910, a patent by Hough (1910) was published that proposed a method of using acidification to precipitate the lignin and resin contained in the BL from the production of alkaline pulp. The precipitated solution was filtered at a high temperature in order to improve the dead-end filtration. Alén *et al.* (1979) published a paper on the precipitation of lignin in which they studied lignin precipitation from softwood BL by introducing carbon dioxide. They found that, when the pressure was increased, the carbonation time was markedly shortened and that the yield was higher. They also reported the strong influence had by the TDS content of the BL on the precipitation yield: the highest precipitation yield of lignin was obtained with a TDS content of 27–30% for softwood BL and 30–35% for hardwood BL (Alén *et al.*, 1985). Uloth and Wearing (Uloth and Wearing, 1989a, 1989b) compared the lignin recovered from three different separation procedures: 1) acid precipitation using sulphuric acid/chlorine dioxide generator waste acid (GWA), 2) carbon dioxide precipitation and 3) ultrafiltration. The conclusion drawn was that, when compared to ultrafiltration, lignin precipitation through acidification provided a higher amount of lignin at a lower estimated cost.

Öhman and Theliander (2006, 2007) have published some papers dealing with kraft lignin precipitation, filtration and washing procedures. They showed that the precipitation pH and temperature are important factors that influence filtration properties. They also concluded that the yield was approximately the same for precipitation performed using strong acid and carbon dioxide. Wallmo *et al.* (2007), who used carbon dioxide to precipitate lignin from BL, found that the chemical composition of the BL affected the total amount of hydrogen ions needed for acidification. They also found that the precipitation yield increased with decreasing temperature and/or increasing TDS content of the BL (Wallmo *et al.*, 2009a). In a later paper, they investigated the influences of mixing speed and hemicellulose content on the filtration properties of BL. Among other things, the results showed that, at a pH above 10.5, the mixing speed affected the rate at which the pH decreased, and that hardwood BL contained a higher concentration of hemicellulose and had a higher average specific filtration resistance in the first filtration step (Wallmo *et al.*, 2009b).

Changing the ionic strength (IS) of lignin solutions is another alternative for lignin precipitation. Villar *et al.* (1996) found that alcohol-calcium solutions were good precipitation agents that recovered 90% of the lignin with good filtration properties. Moreover, Sundin (2000) precipitated lignin in an alkaline solution by the addition of an electrolyte: it was

shown that, in most cases, the critical coagulation concentration of the metal cation increased with increasing pH but decreased with increasing valency of the metal cation.

2.3.2.2 Ultrafiltration

Separating lignin from black liquor by membrane ultrafiltration has also been suggested, and a few studies (Tanistra and Bodzek, 1998, Wallberg *et al.*, 2003, Holmqvist *et al.*, 2005, Jönsson *et al.*, 2008) have been published. These showed that ultrafiltration may be considered as a technically feasible method for producing kraft lignin (Jönsson and Wallberg, 2009, Arkell *et al.*, 2014). When compared with acid precipitation, however, this technique involves greater capital and operating costs (Uloth and Wearing, 1989b). Nevertheless, ultrafiltration is still an interesting option for separating the lignin fraction with a defined molecular weight distribution (Toledano *et al.*, 2010a).

2.3.2.3 The combination of ultrafiltration and acid precipitation

A combination of membrane filtration and precipitation was investigated by Wallmo *et al.* (2009b). It was found that the filtration resistance of precipitated lignin from hardwood black liquor was improved considerably when the concentration of hemicelluloses was lowered prior to precipitation by ultrafiltration.

2.3.2.4 Other methods

Some other methods, such as Sequential Liquid-lignin Recovery Process (SLRP), have been proposed (Lake and Blackburn, 2011, Velez and Thies, 2013) whereby the lignin is acidified by CO_2 at elevated temperatures and pressures (115°C and 6.2 bar). The precipitated lignin fraction is phase-separated as a "liquid lignin" from the aqueous phase via decantation instead of filtration.

2.3.3 The LignoBoost—Separation of lignin from black liquor

As mentioned earlier, lignin precipitation by the acidification of black liquor is not a new technique. Whilst the lignin that is separated in a traditional, single-stage, dewatering/washing process has a relatively low TDS content and high ash content, it also results in severe problems: a complete or partial plugging of the filter cake and/or the filter media. Virtually complete plugging of the filter cakes results in an extremely low flow of wash liquor through the cake, and partial plugging results in high levels of impurities in the lignin. A novel, two-stage washing/dewatering process called "LignoBoost" (Öhman *et al.*, 2007a, 2007b, Theliander, 2008) was developed in order to separate lignin from black liquor efficiently (see Fig. 2.6). A lignin with a low ash content but a high TDS content can be produced on a large industrial scale.
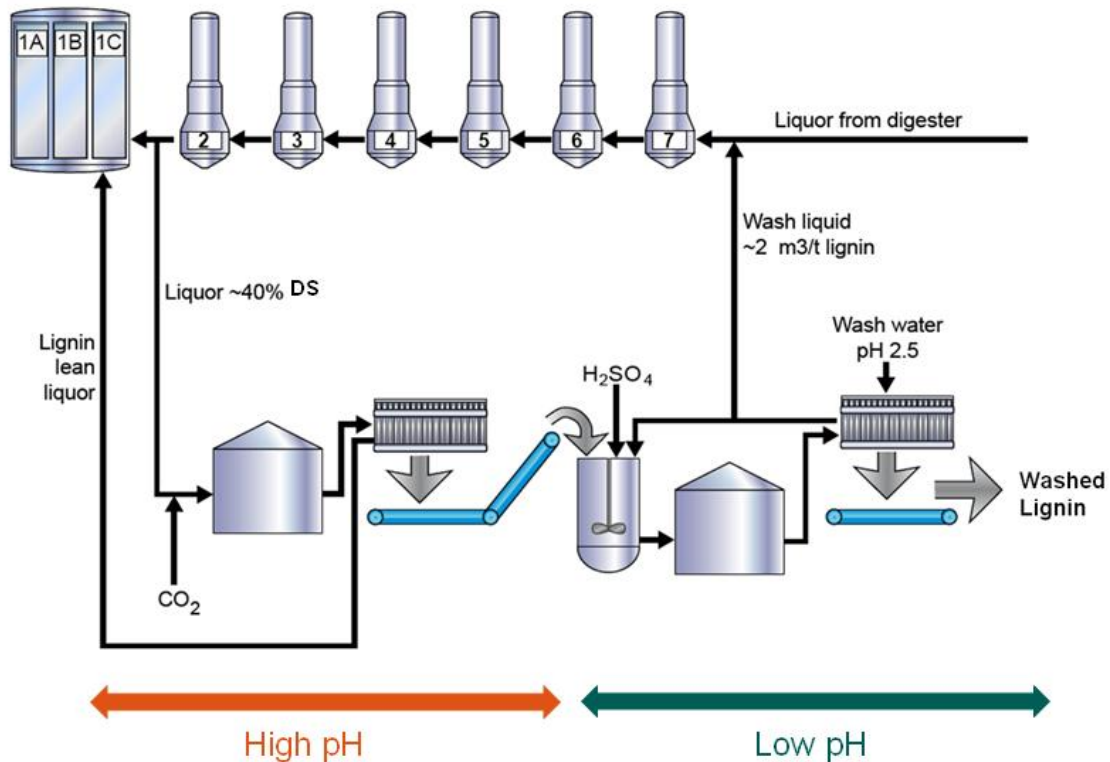
Figure 2.6 Schematic diagram of the LignoBoost process. (Courtesy of Valmet)

In the LignoBoost process, a stream of black liquor is taken from the evaporation plant. The BL is then acidified (preferably with CO_2, pH 10–10.5) at 60–80°C and the lignin is precipitated. The LignoBoost process differs from the single-stage lignin separation process in that the lignin (filter cake) is re-dispersed in the re-slurry tank instead of being washed directly after filtration (Öhman *et al.*, 2007a). When the lignin is re-dispersed, the pH is controlled to approximately the same as the final pH of the washing liquor, *i.e.* pH 2–4, so the concentration gradients of the hydrogen ions during the washing stage are minimized. Therefore the change in the pH and, consequently, in the solubility of the lignin, takes place mainly in the re-dispersing tank and not in the final lignin washing stage. Although gradients of IS are still present, the dilution process in the re-dispersing tank minimizes these changes. The resulting slurry is then filtered and washed by displacement washing.

The major advantages of the LignoBoost process can be regarded as being (Tomani, 2010):

1) Higher yield of lignin.

2) Lignin with lower contents of ash and carbohydrates and higher content of TDS.

3) Lower investment costs due to reductions in the size of the filter area and the volume of acidic washing.

4) Lower operational costs due to a reduction in the amount of H_2SO_4 necessary.

3. THEORY

3.1 Mechanism of lignin precipitation

3.1.1 Kraft lignin in black liquor systems

Kraft lignin macromolecules, as mentioned briefly in Section 2.2, can be considered as being a polyelectrolyte in an aqueous solution (such as BL). They contain weakly acidic groups (mainly phenolic groups on the surface of the molecule) that, in the alkaline condition of BL, become ionized (dissociated); kraft lignin is thus charged and soluble in the solution. A simplified, but reasonable, model of the shape of dissolved kraft lignin is a spherical, amorphous macromolecule (Goring, 1962, Lindström and Westman, 1980) (see Fig. 3.1), where a microgel structure is introduced (Rezanowich and Goring, 1960, Lindström, 1979). The kraft lignin has a compact network core and a loose surface layer where a random, coil-like motion of the macromolecular is possible. The negatively-charged phenolic groups are assumed to be evenly distributed on the surface, or near the surface region, of the lignin molecule (Norgren and Lindström, 2000a), and the surface charge density of the molecule can therefore be assumed to be uniform. The kraft lignin macromolecule is surrounded by a double layer of cations (mainly Na^+ and K^+, distributed according to the Boltzmann distribution).
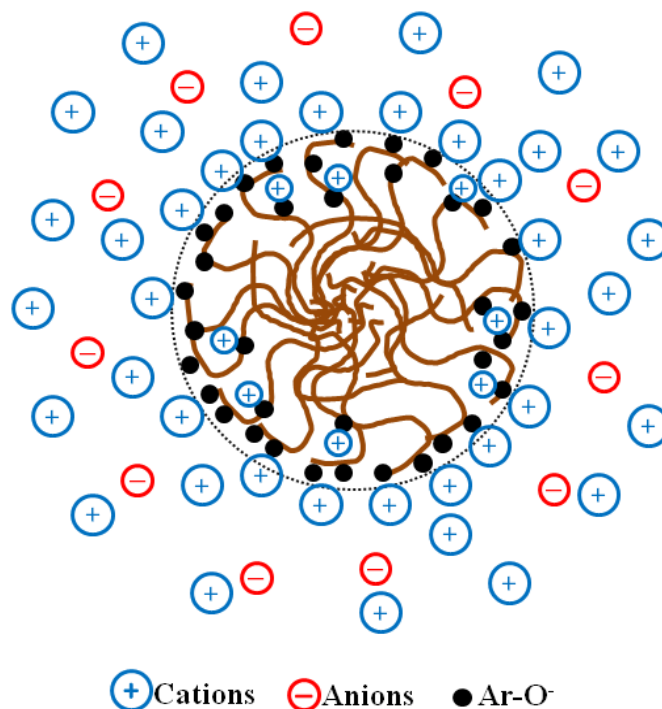

Figure 3.1 An assumed illustration of a kraft lignin macromolecule in an electrolyte solution. Ar-O$^-$ are dissociated phenolic groups. Adapted from Goring (1962).

3.1.2 Lignin precipitation

The first step in the precipitation of kraft lignin by acidification is protonation of the ionized phenolic groups on the lignin macromolecule. The equilibrium of the dissociation/protonation of the phenolic groups on the surface of lignin can be written symbolically as:

$$L - OH_{aq.} \xrightleftharpoons[Protonation]{Dissociation} L - O^- + H^+ \tag{3.1}$$

where L is the lignin macromolecule and –OH is the phenolic group on its surface. The dissociation constant (K_a) of a phenolic group is written as a quotient of the activities of $\{L - OH_{aq.}\}$, $\{L - O^-\}$ and $\{H^+_{surf.}\}$:

$$K_a = \frac{\{L - O^-\}\{H^+_{surf.}\}}{\{L - OH_{aq.}\}} \tag{3.2}$$

The logarithmic constant, pK_a, which equals $-\log_{10} K_a$, is widely used to describe the dissociation of the phenolic groups.

It has been suggested by Marton (1964) and Lindström (1979) that lignin with a high MW behaves like a colloid in aqueous solutions. Self-aggregation of the kraft lignin macromolecules and the precipitation of lignin have been reported in aqueous solutions at room temperature/slightly elevated temperature when the pH is near/below the pK_a of the phenolic groups (Norgren *et al.*, 2001, Norgren *et al.*, 2002). According to the DLVO theory (Shaw, 1993, Evans and Wennerström, 1999), the stability of kraft lignin in solution is an interplay of the attractive and repulsive forces. When the attractive forces, such as van der Waals and other hydrophobic forces dominate, then aggregation is favoured. If, on the other hand, repulsive electrostatic forces between the lignin molecules dominate, the lignin will stay soluble in the solution (Norgren *et al.*, 2001). Rudatin *et al.* (1989) proposed that the balance of these forces is influenced by the structural characteristics of lignin (mainly its MW and functional groups), the conditions of the solution (such as pH, temperature and ionic strength) and the concentration of the lignin.

The precipitation of lignin by acidification in BL can be described as follows: the lignin molecules in BL are negatively charged due to the dissociation of the phenolic groups (and small amounts of carboxyl groups) in alkaline condition and become dissolved. The lignin macromolecules repel each other as a result of the electrostatic repulsive forces, thus making the lignin stable, *i.e.* it remains dissolved in the solution. When the amount of hydrogen ions (H^+) is increased, the H^+ will protonate the negatively-charged phenolic groups on the lignin and neutralize the charges on its molecular surface. The repulsive forces between the lignin molecules are thereby reduced and the attractive forces between molecules become dominant. The lignin molecules start to aggregate and, eventually, the precipitation/coagulation of lignin occurs.

3.2 Poisson-Boltzmann cell model

In a system containing polyelectrolytes (such as lignin) in a solution of electrolytes, the Poisson-Boltzmann (PB) theory may be applied to describe the concentration distribution of

the electrolyte in the system. As mentioned above, in the alkaline conditions prevalent in BL, the negatively-charged surface of the polyelectrolyte (kraft lignin) implies that it has an electrostatic field around it: therefore it will repel other polyelectrolytes of negative charge to various degrees. This makes it reasonable to assume that the concentration of the polyelectrolyte is homogenous in the system and that the Poisson-Boltzmann cell model (PB cell model), in spherical coordinates, is an appropriate model for describing the system. If it is also assumed that the spherical cells are identical and packed together, the system can be described as shown in Fig. 3.2(a). The size of the cell is determined by the overall concentration of polyelectrolytes, which will correspond to a system with cells that overlap somewhat at their boundaries. Each cell contains a concentric, spherical core that represents the polyelectrolyte (Deserno and Holm, 2001). The electrostatic potential ($-F\Phi/RT$) in a cell (regarded as the spherical core in the cell model) is shown in Fig. 3.2(b).
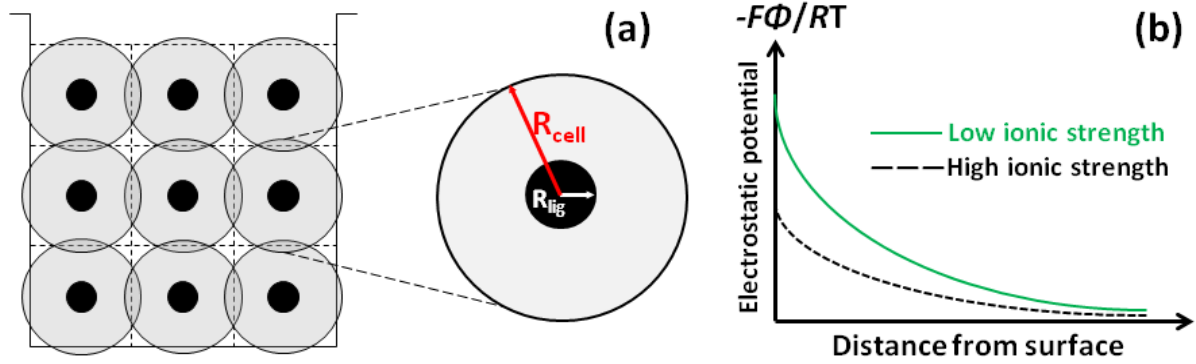

Figure 3.2 (a) An illustration of the Poisson-Boltzmann (PB) cell model in spherical symmetry. (b) The profile of the electrostatic potential of a lignin molecule.

The classic PB equation can be applied to express the relationship between the electrostatic potential and the concentration of the ionic species, which is obtained from the Boltzmann distribution of electrolytes (Eq. 3.3) and Poisson's equation (Eq. 3.4).

$$c_i(r) = c_i(R_{cell})\exp\left(-\frac{z_i F\Phi(r)}{RT}\right) \tag{3.3}$$

$$\nabla^2\Phi(r) = -\frac{\rho(r)}{\varepsilon_0\varepsilon_r} = -\frac{F}{\varepsilon_0\varepsilon_r}\sum_i z_i c_i(r) \tag{3.4}$$

Substituting Eq. 3.3 into Eq. 3.4 yields the PB equation in Eq. 3.5 together with suitable boundary conditions (Gunnarsson *et al.*, 1980, Norgren and Lindström, 2000a):

$$\nabla^2\Phi(r) = -\frac{F}{\varepsilon_0\varepsilon_r}\sum_i z_i c_i(R_{cell})\exp\left(-\frac{z_i F\Phi(r)}{RT}\right)$$

Boundary conditions: $\left.\frac{d\Phi}{dr}\right|_{r=R_{lig.}} = -\frac{\sigma}{\varepsilon_0\varepsilon_r}$, $\left.\frac{d\Phi}{dr}\right|_{r=R_{cell}} = 0$ $\tag{3.5}$

where ρ (C m^{-3}) is the volumetric charge density, F (C mole^{-1}) is the Faradays constant, R (J mole^{-1} K^{-1}) is the ideal gas constant, T (Kelvin) is the absolute temperature, c_i (mole m^{-3}) is the concentration of an electrolyte, i and Φ (V) is the electrostatic potential. R_{cell} and $R_{lig.}$ are the radii of the cell and the lignin polyelectrolyte, respectively. $c_i(R_{cell})$ represents the

concentration of electrolyte, i, in the bulk solution. z_i is the valence number of the electrolyte, and ε_0 and ε_r are the permittivity in vacuum and the relative permittivity of the liquid, respectively.

The Poisson-Boltzmann approach is restricted to dilute electrolyte solutions since no interactions between the electrolytes are accounted for. Delville (1984) proposed a modification of the classic PB equation and expressed the Boltzmann distribution of electrolytes in activities, $a_i(r) = \gamma_i c_i$ (mole m^{-3}), in Eq. 3.6.

$$a_i(r) = \gamma_i(R_{cell})c_i(R_{cell}) \exp\left(-\frac{F\Phi(r)}{RT}\right) \tag{3.6}$$

Thus, the effect of the non-ideal, entropic reallocation of the electrolytes arising from the interionic interactions is described by the activity coefficients. Such interionic interactions may, for example, be columbic interactions (assumed to be the most dominant) and finite size-induced repulsion of ions (Pitzer, 1991).

The Pitzer method is useful for determining the activity coefficients of multicomponent systems of electrolytes in solutions with a high IS. Further details of this method can be found in the literature (Pitzer, 1991) and in Paper V.

If the classic Poisson equation, Eq. 3.4, is combined with Eq. 3.6, a modified Poisson-Boltzmann equation, Eq. 3.7, is achieved.

$$\nabla^2\Phi(r) = -\frac{F}{\varepsilon_0\varepsilon_r}\sum_i z_i \frac{\gamma_i(R_{cell})}{\gamma_i(r)}c_i(R_{cell}) \exp\left(-\frac{z_iF\Phi(r)}{RT}\right)$$

Boundary conditions: $\left.\dfrac{d\Phi}{dr}\right|_{r=R_{lig.}} = -\dfrac{\sigma}{\varepsilon_0\varepsilon_r}$, $\left.\dfrac{d\Phi}{dr}\right|_{r=R_{cell}} = 0$ $\tag{3.7}$

In Eq. 3.7 the volumetric charge density, at a distance r from the electrolyte cell's centre point for electrolyte, i, scales with the ratio of the activity coefficient at the outer boundary of the cell and at a distance r. The effect of non-ideal interactions between electrolytes on the volumetric charge density is described in the ratio and thereby also in the electrostatic potential. Eq. 3.7 may possibly be better at predicting the distribution profile of the electrolyte's concentration at a higher IS than the classical Poisson-Boltzmann model, since it accounts for non-ideal interionic interactions.

3.3 Calculation of the dissociation degree of phenolic groups

The phenolic groups on the lignin molecule are dissociated under high alkali conditions, as mentioned in Section 3.1. The dissociation degree, α, of the phenolic groups can be obtained by using the PB cell programme developed by Jönsson (2003) and is based on the classic Poisson-Boltzmann equation (Eq. 3.5). However, the electrolyte solution conditions in this study are of high IS. Moreover, the surface charge density when all of the phenolic groups are dissociated (σ_0) is very low, being approximately -0.03 C m^{-2} for lignin molecules larger than 1 kDa (Norgren *et al.*, 2001) and the concentration gradient of the electrolytes in the cell model is expected to be rather low. The activity coefficients of the electrolytes are strongly dependent on the temperature (see Paper V) and concentration of the electrolytes. If the temperature in the cell is considered as being constant with respect to r and the concentration

gradient of the electrolytes are assumed to be rather low, the ratio $\gamma_i(R_{cell})/\gamma_i(r)$ in Eq. 3.7 may be assumed to be approximately unity, and the modified PB equation (Eq. 3.7) can be simplified to the classic Poisson-Boltzmann equation given in Eq. 3.5. Thus the PB cell programme can be used even for non-ideal cases if the surface charge density is sufficiently low and the ionic strength is sufficiently high, *e.g.* a black liquor systems. In this study, the ratio $\gamma_i(R_{cell})/\gamma_i(r)$ was found to be close to unity, see Paper V.

The dissociation degree of phenolic groups, α, is defined in Eq. 3.8.

$$\alpha = \frac{[L-O^-]}{[L-O^-]+[L-OH_{aq.}]} \tag{3.8}$$

$[L-O^-]$ and $[L-OH_{aq.}]$ are the concentrations (mole kg^{-1} liq.) of dissociated and protonated phenolic groups on the surfaces of the lignin molecules in the BL solution, respectively.

Combining Eq. 3.2 and 3.8 yields Eq. 3.9:

$$K_a = \frac{\gamma_{L-O^-}}{\gamma_{L-OH}} \frac{\alpha}{1-\alpha} \{H^+_{surf.}\} \tag{3.9}$$

where γ_{L-O^-} and γ_{L-OH} are the activity coefficients of the dissociated and protonated phenolic groups, respectively, and $\{H^+_{surf.}\}$ is the activity of protons in the vicinity of the lignin molecule's surface. In order to estimate the equilibrium constant (K_a) in Eq. 3.9 it is thus necessity to predict the concentration of protons at the surface of the lignin molecule, which is dependent on the electrostatic potential of the cell. Moreover, the potential is dependent on α, since the density of the surface charge is dependent on the degree of dissociation of the phenolic groups. For this reason it is necessary to calculate α in an iterative manner for a given condition. The calculation algorithm for estimating α is illustrated in Fig. 3.3, with the steps being described beneath it.
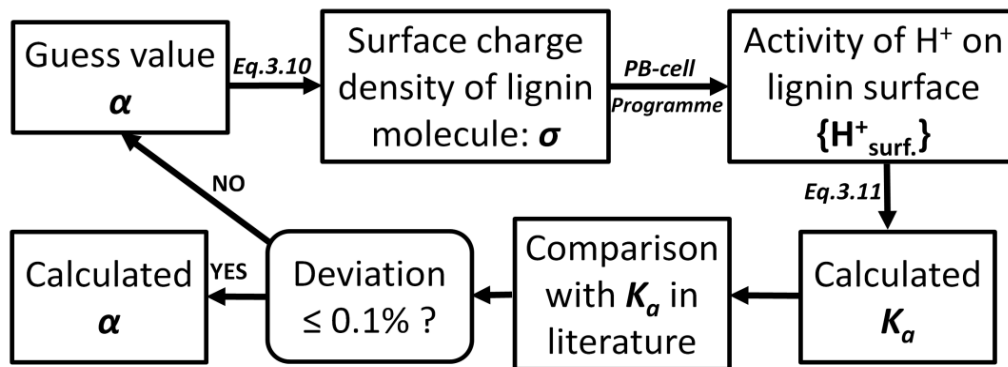

Figure 3.3 The algorithm used in this study to calculate α.

1) α is given a guess value.

2) The average surface charge density of a lignin molecule is expressed according to Eq. 3.10, where σ_0 (C m^{-2}) is the surface density of totally dissociated phenolic groups.

$$\sigma = \alpha\sigma_0 \tag{3.10}$$

3) The activity of the hydrogen ions on the surface of a lignin molecule $\{H_{surf.}^+\}$ is calculated by the PB cell programme, an example of which is given in Appendix I.

4) K_a is estimated by assuming both the activity coefficients of dissociated lignin (γ_{L-O^-}) and protonized lignin (γ_{L-OH}) to be unity. Consequently, Eq. 3.9 can be reduced to Eq. 3.11.

$$K_a = \frac{\alpha}{1-\alpha}\{H_{surf.}^+\} \tag{3.11}$$

5) The predicted equilibrium constant (K_a) in Eq. 3.11 is justified through comparison with values in literature. Norgren and Lindström (2000a) suggest that the pK_a for phenolic groups on the molecule surface of a strongly screened softwood kraft lignin is that of the monomeric coniferyl alcohol, *i.e.* 10.2, at 25°C. The temperature dependence of K_a was accounted for using the Van 't Hoff equation, Eq. 3.12.

$$\frac{d\ln K_a}{d(1/T)} = -\frac{\Delta H}{R} \tag{3.12}$$

where the constant dissociation enthalpy (ΔH) is assumed to 20.0 kJ mole^{-1} for phenol (Zavitsas, 1967). After temperature adjustment (1.2×10^{-10} at 45°C and 1.9×10^{-10} at 65°C) from values found in the literature, K_a is then compared with the estimated K_a that is based on the guessed α.

6) A correct value of α that corresponds to the literature value is obtained by reiteration until the deviation in the calculated K_a is less than 0.1%.

4. MATERIALS AND METHODS

4.1 Raw material (Papers I - IV)

Papers I & II:

The mixed hardwood/softwood black liquor (denoted HS) used in Papers I and II was obtained from a batch kraft pulp mill that produces bleachable grade pulp on two fibre lines. The wood chips used by the mill are approximately 1/3 softwood (a mixture of Scots pine and Norway spruce) and 2/3 hardwood (mainly birch). The black liquors from the two fibre lines are mixed prior to entering the chemical recovery department. The total dry solid (TDS) content of the HS was approx. 33.2% in the precipitation experiments.

Paper III:

The softwood black liquor (denoted S0) used in Papers III and IV was obtained from another batch kraft pulp mill, in which 80% spruce and 20% pine are used to produce pulps. The sodium/potassium concentration was adjusted by adding de-ionized water (from 3.30 mole kg^{-1} liq. to 2.87 mole kg^{-1} liq.) so that it would be possible to compare the results with those obtained in Papers I and II. The TDS of the S0 was approx. 32% in the precipitation experiments.

Paper IV:

The original black liquor was the same S0 as used in Paper III but it had been fractionated by cross-flow membrane filtration. Four BL fractions, *i.e.* F1, F2, F3 and F4, were achieved with a TDS of 29.9%, 29.3%, 29.9% and 24.1%, respectively.

4.2 Cross-flow membrane filtration (Paper IV)

Cross-flow filtration (ultra/nanofiltration) was performed using a bench-scale membrane apparatus. The system consisted of a 30 L tank, a gear pump and a membrane unit Kerasep^{TM} (Novasep, Pompay, France). The ceramic membranes were made of TiO_2 coated with ZrO_2 and the surface area was 816 cm^2. The operational pH range was 0–14 and the trans-membrane pressure range was 0–0.6 MPa; the membrane used was temperature-stable up to 100°C. Three sets of membranes were used, with a Molecular Weight Cut-Off (MWCO) of 1, 5 and 15 kDa, respectively. All experiments were carried out with a total re-circulation of the BL at approx. 40°C. The trans-membrane pressure was approx. 0.35 MPa and the flow rate was approx. 35.5 L min^{-1}.

A starting volume of 24.5 L of softwood black liquor (S0) was processed according to Fig. 4.1. A 15 kDa membrane was used in the first ultrafiltration step, which resulted in a volume reduction (VR, calculated as volume of permeate divided by volume of initial feed) of 0.76 and a volume reduction factor (VRF, calculated as initial feed volume divided by retentate volume) of 4.2. In the second step, the permeate from the first step was fractionated continuously via a 5 kDa cut-off membrane, which resulted in a VR and VRF of 0.73 and 3.7, respectively. In the third and final step, the permeate from the previous step was fractionated

further via a 1 kDa cut-off membrane (nanofiltration) with a VR of 0.7 and a VRF of 3.4. Four samples of black liquor were collected: Fractions 1–3 (F1, F2 and F3) were the retentate after each fractionation step, whilst Fraction 4 (F4) was the permeate after fractionation with the 1 kDa cut-off membrane. All fractions were stored at 4°C.
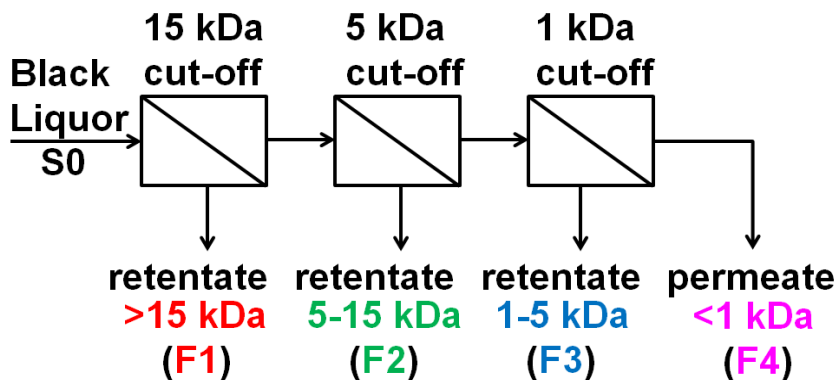

Figure 4.1 Schematic diagram of the cross-flow filtration experiments.

4.3 Precipitation of lignin (Papers I to IV)

The precipitation experiments for all of the black liquor samples (HS, S0, F1, F2, F3 and F4) were carried out on laboratory scale following the methodology shown in Fig. 4.2.

A sample of black liquor was weighed (100 or 200 g) and placed in a plastic bottle with a magnetic stirrer to enhance mixing when the bottle was shaken; a certain amount of sodium sulphate (Fisher Scientific, 99.5%) was added if a higher IS was required. The bottle was closed with a lid and placed in a water bath for 1 hour in order to reach the target temperature, with the bottle being shaken well every 10 minutes. The temperature ranged from 45°C to 75°C and, when the target temperature was reached, 6M H_2SO_4 was added to reach the target pH. The pH measurement was performed at room temperature using a JENWAY Model 370 pH/mV Meter with temperature correction. The electrode used was an Epoxy bodied combination pH electrode (924 005) suitable for pH measurement between 10°C and 105°C. A three-point calibration at pH values of 7.00, 10.00 and 12.00 was performed prior to the measurements. The pOH value at the corresponding temperature is calculated by:

$$pOH = pK_w(T) - pH \tag{4.1}$$

where T is the corresponding temperature when the solution is measured. The calculation equation for $pK_w(T)$ can be found in the literature (Whitfield, 1975).

The bottle was then shaken every 10 minutes for 1 hour to obtain an apparent equilibrium. When precipitation was complete, the sample was filtrated through a Büchner funnel with a Munktell, grade 5 filter paper. The filtrate was collected and stored in a gas tight bottle, ready for the lignin and carbohydrate analyses. The filter cake, which is the precipitated lignin (a dark-coloured solid), was then washed with a solution of pH 3 (de-ionized water with the addition of H_2SO_4) except for in Paper II, where the wash water was adjust to the same pH

and IS as in the precipitation process. Finally, it was dried at 105°C for 8 hours. Detailed experimental parameters for the various samples of BL are given in Table 4.1.
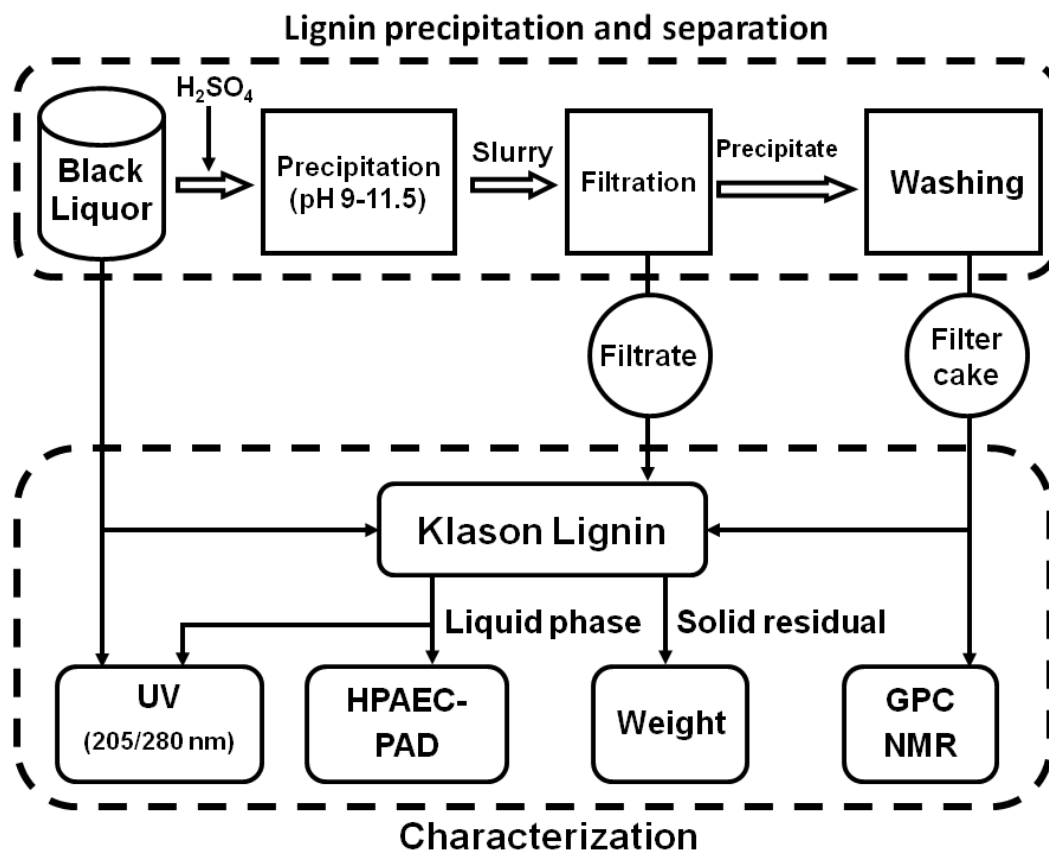

Figure 4.2 Schematic diagram of the acidification of the black liquor, the filtration processes and the characterization units.

Table 4.1 Experimental parameters of the lignin precipitated in the various BL samples.

Paper	BL type	TDS (%)	pH						T (°C)					IS addition (%)				
			11.5	11	10.5	10	9.5	9	80	75	65	55	45	0	5	10	15	20
I	HS	33.2		√	√	√	√			√	√	√	√	√	√		√		√
II			√	√	√	√	√		√	√	√	√	√	√	√	√	√	√
III	S0	32.0		√	√	√	√			√		√	√	√		√		√
IV	F1	29.9	√	√			√				√		√	√				√
	F2	29.3			√	√	√				√		√	√				√
	F3	29.9			√	√	√				√		√	√				√
	F4	24.1			√		√	√			√		√	√				√

4.4 Analytical methods (Papers I-V)

4.4.1 Properties of black liquor

The total dry solids (TDS) content of the black liquor was determined according to the Tappi T650 om–09 method: the sample was dried at 105°C for 24 hours and the experimental

deviation was found to be ±0.6%. The concentrations of NaOH and Na_2S were measured according to the titration method proposed by Wilson (1968). The errors in measurement of the NaOH and Na_2S contents were ±0.6% and ±2.2%, respectively. After wet combustion in a microwave oven, the concentrations of Na and K in the black liquor were measured by atomic absorption spectroscopy (AAS) (Thermoscientific iCE 3000), with the errors of measurement being ±1.6% and ±6.0%, respectively. The concentration of lignin was determined by UV light absorption using a Specord 205, Analytik Jena, with a wavelength of 280 nm. The absorption constant for softwood lignin was 24.6 dm^3 g^{-1} cm^{-1} (Fengel *et al*. 1981). The experimental error of the UV measurements was estimated as being ±0.9%.

The concentrations of the anions in the black liquor, *i.e.* Cl^-, SO_4^{2-}, SO_3^{2-}, and $S_2O_3^{2-}$, were determined by ion chromatography (IC) in this study: the system used consisted of an ion chromatograph instrument (850 Professional IC, Metrohm with Metrosep A Supp7 columns). The samples were filtered through 0.45 μm PVDF membrane syringe filters prior to injection, and the system was run at a flow rate of 0.8 mL min^{-1} with sodium carbonate (3.6 mM) as the eluent. The concentrations of the anions were calculated according to standard calibration for each anion. Three different concentration points for each anion were chosen: Cl^- with 10–50 mg L^{-1}, SO_4^{2-} with 50–150 mg L^{-1}, SO_3^{2-} with 10–50 mg L^{-1} and $S_2O_3^{2-}$ with 56–140 mg L^{-1}. The standard deviation was ±1.5% based on the calibration curves of standard solutions.

4.4.2 Klason lignin

Klason lignin is defined as the solid residual material that is obtained after a sample of BL has been subjected to hydrolysis treatment with 72% H_2SO_4. The method used, as presented by Theander and Westerlund (1986), can be summarized as follows: either 0.2 g of an oven-dried precipitated sample of lignin or 1.2 g of filtrated liquor is weighed and 3 mL of 72% H_2SO_4 is added to the sample. The sample is then evacuated for 15 min and placed in a water bath at 30°C for 1 hour, after which 84 g of deionized water is added and it is heated to 125°C in an autoclave for 1 hour. After hydrolysis, the sample is filtrated and the insoluble solid residue, which is referred to as Klason lignin, is measured gravimetrically according to the Tappi T222 cm–00 method. The experimental deviation of Klason lignin concentration was estimated to be ±3%.

4.4.3 Acid-soluble lignin (ASL)

The filtrate from Klason lignin method was diluted to 100 mL in a volumetric flask. A solution that was 50 (for precipitated lignin) or 100 (for black liquor filtrate) times weaker was prepared for UV measurement. The concentration of acid-soluble lignin was measured based on the absorbance value determined by UV at a wavelength of 205 nm in a Specord 205, Analytik Jena. The absorption constant used was 110 dm^3 g^{-1} cm^{-1} (Dence, 1992) and the deviation of the results was estimated to be ±0.9%.

4.4.4 Analysis of carbohydrates

The filtrate form Klason lignin method is also used for the analysis of carbohydrate. Firstly the filtrate was diluted to 100 mL, as for ASL. This solution was further diluted 5 times and filtered through a 0.45 μm PVDF filter prior to measurement. Fucose is used as an internal

standard for the following High-Performance Anion Exchange Chromatography with Pulsed Amperometric Detection (HPAEC-PAD) measurement.

In Paper I, the HPAEC-PAD instrument employed was a Varian Pro-Star High Performance Liquid Chromatography (HPLC) equipped with an AutoSampler Model 410 and a Dionex Isocratic Pump IP20; the detector was an Electrochemical Detector, Varian Star 9080. The running system consisted of two Dionex columns: a pre-column CarboPac™ PA 1 (2×50 mm) and a main column CarboPac™ PA 1 (2×250 mm). The software used was the Star Chromatography Workstation, System Control Version 5.50 by Varian. A flow rate of 2 mL min^{-1} was applied to all samples, and the standard concentration of fucose was 40 mg L^{-1}. The estimated error of determination is about 6% based on the calibration curve of standard samples.

In Papers II, III and IV, the analysis of monomeric sugars was performed using the Dionex ICS–5000 HPLC system equipped with CarboPac PA1 columns and run using NaOH, NaOH/NaAc (0.2 M) as the eluents. An Electrochemical Detector was used for detection measurements. The software used was Chromeleon 7, Chromatography Data System, Version 7.1.0.898.

The amounts of carbohydrates analyzed were corrected for the acid hydrolysis yield (Janson, 1974) which varies for different sugars; the values used were collected from experimental results reported by Wigell *et al.* (2007). The amounts of xylan and (galacto)glucomannan were calculated using the algorithm described in Appendix II.

4.4.5 Molecular weight (MW) and molecular weight distribution (MWD)

The molecular weight (MW) of lignin in the BL was measured by first acidifying the black liquor to pH 2.5 at 45°C. The resulting lignin precipitate was separated and, as the filtrate solution was clear, it was assumed that the lignin had precipitated completely.

The MW of the precipitated lignin was determined by Gel Permeation Chromatography (GPC), which provides a rapid way of obtaining information of the MW of polymers. In this study, the dried precipitated lignin sample was dissolved in dimethyl sulphoxide (DMSO)/LiBr (10 mM) to a concentration of 0.25 g L^{-1}. The resulting solution was then analyzed in a GPC to obtain the average molecular weight as well as the molecular weight distribution of the precipitated lignin.

The measurement was performed on a PL-GPC 50 Plus Integrated GPC System from Polymer Laboratories (Varian Inc. Company) equipped with a detection system consisting of a refractive index (RI) and Ultraviolet (UV) detector. The UV measurements were performed at a wavelength of 280 nm, which is generally associated with lignin, and the RI responses corresponded to both lignin and carbohydrates.

The system was equipped with two PolarGel-M (300×7.5 mm) columns and a PolarGel-MGuard column (50×7.5 mm). The mobile phase was DMSO with the addition of 10 mM LiBr, with the sample being injected via a PL-AS RT GPC Autosampler at a flow rate of 0.5 mL min^{-1}. The sample was analyzed using software Cirrus GPC Version 3.2. Pullulan of nine

different molecular weights (708, 375, 200, 107, 47.1, 21.1, 5.9, 0.667 and 0.18 kDa) was employed for calibration (Polysaccharide Calibration Kit, PL2090–0100, Varian). The estimated error of determination is about 5% based on the calibration curve of standard samples. All the results obtained were baseline corrected.

4.4.6 Determination of functional groups

Nuclear Magnetic Resonance (NMR) measurements were performed in order to analyze the content of functional groups in the precipitated lignin. The samples were acetylated according to Lundquist (1992b), whereby 1–2 ml of acetic anhydride (EMSURE, ACS, ISO, Reag. Ph Eur grade)/pyridine (EMSURE, ACS. Reag. Ph Eur grade) (1:1, v/v) is added to approx. 100 mg of precipitated lignin in a 50-ml flask at room temperature and left overnight. After acetylation, 25 mL of ethanol (SOLVECO, 99.5%) is added and the solvents are removed via rotary evaporation during a period of 30 min. The repeated addition and removal (rotary evaporation) of ethanol (between five and ten times) results in the removal of acetic acid and pyridine from the sample. Finally, the acetylated lignin is dried in a desiccator over KOH and P_2O_5.

In this study, a 50 mg sample of acetylated lignin was dissolved in 0.5 ml DMSO-d_6 (ARMAR Chemicals, 99.8%). ^{1}H and ^{13}C NMR spectra were recorded at 25ºC on a Bruker Avance III HD 18.8 T NMR spectrometer equipped with a 5 mm TCI Cryoprobe (cold ^{1}H and ^{13}C channels) operating at a frequency of 800 MHz for ^{1}H and 201 MHz for ^{13}C detection. The ^{1}H spectra were recorded with a 90° pulse angle, 5 s pulse delay, 1024 scans and 2.56 s acquisition time. The ^{13}C spectra were recorded with an inverse-gated decoupling sequence, 90° pulse angle, 12 s pulse delay, 3200 scans and 1.36 s acquisition time. The resulting spectra were baseline corrected and the data was processed by MestreNove (Mestrelab Research). The standard deviation, estimated by Landucci (1985), Pu and Ragauskas (2005), is 3.0%.

5. RESULTS AND DISCUSSION

5.1 Characterization of black liquor (Papers I-IV)

The chemical analysis of the BL examined is presented in Table 5.1. The properties of BL are related to both the raw material and the process conditions in the pulp mills that produce them and, consequently, some of the characteristics of hardwood BL and softwood BL differ. It should also be kept in mind that, as in most other studies, the result of the MW measurements of lignin obtained in this study, *i.e.* GPC analysis, is a relative value. The measured value is correlated to many factors, such as the separation column, the eluent used, the calibration standard and the operation temperature. It means that different values could be achieved using another GPC system. All the MWs in this study have, however, been determined using the same protocol, thus allowing a relative comparison to be made.

5.1.1 Molecular weight of lignin

It can be seen in Table 5.1 that the weight-average molecular weight (M_w) of kraft lignin from S0 is higher than that from HS, which may be the result of there being a large proportion of hardwood lignin in HS. Hardwood lignin contains many β-O-4 linkages (Larsson and Miksche, 1971, Sjöström, 1993) that become heavily degraded during kraft cooking, and this may result in lignin fragments with lower MWs. Softwood (G-type) lignins contain larger amounts of C-C bonds (Table 2.1): these bonds are more stable during kraft cooking. Softwood lignin also contains more reactive C_5 positions in the aromatic ring, which is more favourable for condensation reactions (Gierer, 1980, Chakar and Ragauskas, 2004). The MW of softwood kraft lignin is therefore higher than that of hardwood kraft lignin.

It can also be seen that the MW of different lignin fractions decreases from F1 to F4. The polydispersity (PD) of lignin fractions F2, F3 and F4 becomes much smaller than that of the lignin from S0, which indicates that the lignin in these fractions has a narrower molecular weight distribution (MWD) (see Fig. 5.1) and is, thus, more homogenous. Fraction F1 has about the same PD as S0: this is expected, since all molecular weights are represented in this fraction. One interesting observation is that the MW of lignin from F3 is slightly higher than 5 kDa and that from F4 is higher than 1 kDa. This might be explained by the fact that the MWCO of the membrane provided by the manufacturer was measured using a standard method that differs from the MW analysis of lignin used in this work. Another possible reason is that the lignin molecules have different structures (*e.g.* some are linear and others are more globular (Vainio *et al.*, 2004)) and they may pass through a membrane with a smaller MWCO. Moreover, the MWD curve of the lignin (Fig. 5.1, UV response) in F4 shows several peaks in the low MW region, indicating the presence of low MW fragments such as mono-/dimmers of lignin (Sevastyanova *et al.*, 2014).

Table 5.1 Some important characteristics of the black liquor samples.

Black liquor types			Papers I & II	Paper III	Paper IV			
			HS[§]	S0[*]	F1[★]	F2[†]	F3[‡]	F4[▲]
Molecular weight cut-off (kDa)			#	#	>15	5–15	1–5	<1
Molecular weight (kDa)	RI	M_w	10.7	13.5	20.2	8.9	8.2	4.5
		M_n	6.2	6.4	10.8	5.6	5.4	3.4
		PD	1.7	2.1	1.9	1.6	1.5	1.3
	UV	M_w	9.0	11.8	18.6	7.2	6.6	2.9
		M_n	1.0	1.4	2.1	1.1	1.2	0.6
		PD	9.0	8.4	8.9	6.5	5.5	4.8
Dry Content	(%)		33.2	32	29.9	29.3	29.9	24.1
[Na]	(mole kg^{-1} liq.)		2.76	2.67	2.51	2.44	2.47	2.44
[K]			0.11	0.20	0.10	0.19	0.20	0.20
[Na]+[K]			2.87	2.87	2.62	2.62	2.68	2.64
Klason lignin	(g kg^{-1} liq.)		88.9	98.8	112.4	82.8	93.6	19.0
Acid-soluble lignin			28.2	24.0	10.6	25.8	25.8	26.0
Total lignin			117.1	122.8	123.0	108.6	119.4	45.0
GGM			2.38	2.20	2.55	1.53	1.61	0.84
Xylan			6.07	2.83	3.69	2.18	2.12	0.47
Total carbohydrates			8.93	5.55	6.90	4.01	4.05	1.49
NaOH			12.9	11.2	7.5	14.2	12.8	13.8
Na$_2$S			13.2	14.7	0.7	4.8	2.7	5.5
Cl$^-$	(g kg^{-1} TDS)		2.43	1.60	1.12	2.48	2.37	3.37
SO$_4^{2-}$			17.2	35.3	213.5	30.5	30.1	45.0
SO$_3^{2-}$			13.5	28.2	9.2	26.1	25.0	39.1
S$_2$O$_3^{2-}$			37.8	25.6	13.9	46.1	46.3	67.3

§HS: Mixed hardwood/softwood black liquor; *S0: Unfractionated softwood black liquor; ★F1: Fractionated softwood black liquor, Fraction 1; †F2: Fractionated softwood black liquor, Fraction 2; ‡F3: Fractionated softwood black liquor, Fraction 3; ▲F4: Fractionated softwood black liquor, Fraction 4.
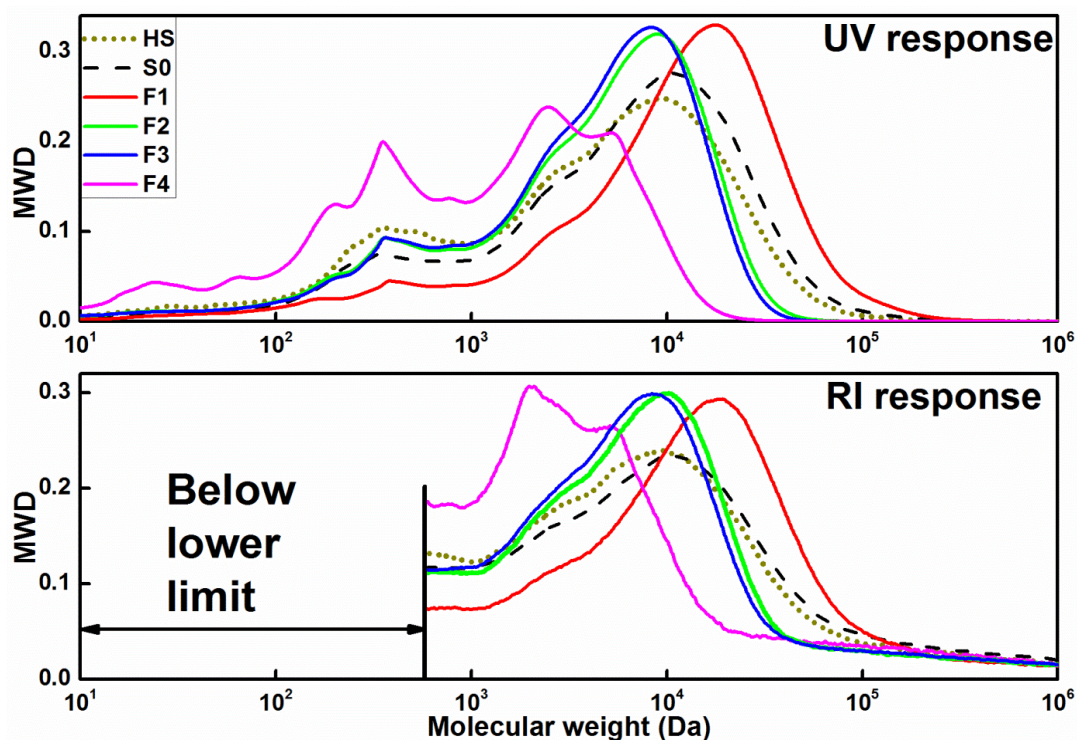
Figure 5.1 Molecular weight distribution (MWD) of the lignin obtained from the softwood black liquor and its four fractions and the mixed hardwood/softwood black liquor.

5.1.2 Functional groups

13C NMR

The analysis of the functional groups of the lignins in S0 and its fractions and HS was performed by NMR spectroscopy. The ^{13}C NMR spectra of acetylated lignin are presented in Fig. 5.2. Chemical shift assignments of lignin moieties are according to the literature (Kringstad and Roland, 1983, Mörck and Kringstad, 1985, Mörck *et al.*, 1986, Faix *et al.*, 1994) and a quantitative comparison is summarized in Table 5.2. The aromatic region (106–154 ppm for softwood and 102–160 ppm for hardwood kraft lignin) was integrated and calibrated to six, which represents six aromatic carbons (Landucci *et al.*, 1998, Ralph and Landucci, 2010, Choi and Faix, 2011, Wells Jr *et al.*, 2013, Min *et al.*, 2013). Quantitative evaluation of the functional groups and carbohydrates was then calculated as follows:

$$\text{Number of carbons (per } C_9 \text{ unit)}=6 \times \frac{\text{integrated area of individual functional group}}{\text{integrated area of aromatic carbon}} \qquad (5.1)$$

The signals from the region 166–171.3 ppm represent the hydroxyl groups on lignin (acetylated form), see Fig. 5.2. More specifically, they are primary (OH$_{pri.}$) aliphatic, secondary (OH$_{sec.}$) aliphatic and phenolic (OH$_{phen.}$) hydroxyl groups. As can be seen in Table 5.2, the amount of OH$_{phen.}$ of kraft lignin is higher than that of the native lignin (Table 2.2), which indicates that the aryl-ether bond of the native lignin has been cleaved, and that more free phenolic groups have been formed. Moreover, Table 2.2 shows that although native hardwood lignin contains equal, or lesser, amounts of phenolic groups than native softwood

29

lignin, the phenolic content of kraft lignin derived from HS is nevertheless higher than that from S0. This is most likely due to the hardwood lignin being degraded more heavily (as discussed in Sections 2.1.3 and 5.1.1), which results in more OH$_{phen.}$ groups being formed. An increasing amount of OH$_{phen.}$ of lignin is also found from F1 to F4, whilst the MW of lignin decreases from F1 to F4. In these fractions it can be seen that the content of aliphatic hydroxyl groups is much lower than phenolic groups, which is in agreement with previous studies of softwood kraft lignin (Robert *et al.*, 1984, Mörck and Kringstad, 1985). Lesser amounts of OH$_{pri.}$ indicate the terminal elimination of hydroxylmethyl groups, *i.e.* cleavage of the lignin side chain, and a lower OH$_{sec.}$ content indicates the formation of unsaturated/condensed structures. Moreover, the content of hydroxyl groups in F1 differs from that in the other three fractions, which could indicate that the aryl ether linkages and side chains of lignin with higher MWs in F1 are not heavily cleaved.

The signal of methoxyl (OMe) group is shown at δ_C 54–57.5 ppm. In Table 5.2 it can be seen that hardwood kraft lignin contains higher amounts of OMe groups than softwood kraft lignin, which is mainly due to the S-type of lignin present in hardwood. Moreover, the OMe content in the lignin in fractions F1 to F4 decreases with decreasing MW of the lignin, which is in agreement with previous studies (Wada *et al.*, 1962, Lin and Detroit, 1981, Mörck *et al.*, 1986, Lin, 1992). This can be due to the demethylation of methyl-aryl ether linkages on the aromatic ring of small kraft lignin molecules, as mentioned in Section 2.1.3. The overall OMe content of kraft lignin reported in Table 5.2 is also lower than the native lignin (Table 2.2), which is a result of the reaction mentioned above.

Table 5.2 Quantitative analysis of softwood kraft lignin from each black liquor fraction based on ^{13}C NMR and ^{1}H NMR spectra. (All values are calculated on a 100 C$_9$ basis, using lignin obtained as described in Section 4.4.5.)

Lignin in BL	^{13}C-NMR					^{1}H-NMR		
	Ac. OH$_{phen.}$	Ac. OH$_{sec.}$	Ac. OH$_{pri.}$	Xyl$_{C1}$	OMe	Ac. OH$_{ali.}$	Ac. OH$_{phen.}$	OMe
	166–168.8 ppm	168.8–169.5 ppm	169.5–171.3 ppm	100–102 ppm	54–57.5 ppm	1.75–2.1 ppm	2.1–2.4 ppm	3.3–4.0 ppm
HS	94	16	23	4	103	194	254	418
S0	87	16	25	3	80	214	214	373
F1	78	21	33	6	86	252	176	433
F2	90	14	23	1	78	197	238	327
F3	93	13	23	1	74	176	242	321
F4	99	13	23	N/A	67	141	275	315

It is known that the kraft lignin in the later stages of cooking contains greater amounts of carbohydrates that might be bonded to it in the form of LCC structures (Gellerstedt and Lindfors, 1984). One of the carbohydrate constituents appears to be xylan: the signal of xylan carbons in ^{13}C NMR spectra is assigned as Xyl$_{C1}$ (100–102 ppm) (Kringstad and Roland, 1983,

Mörck *et al.*, 1986). The concentrations of the carbohydrates (mainly xylan) in this study were analyzed by ^{13}C NMR (Table 5.2) and the results that were obtained are in accordance with the characterization of the black liquor fractions given in Table 5.1, *i.e.* that the softwood lignin fraction with a higher MW contains a greater amount of carbohydrates.
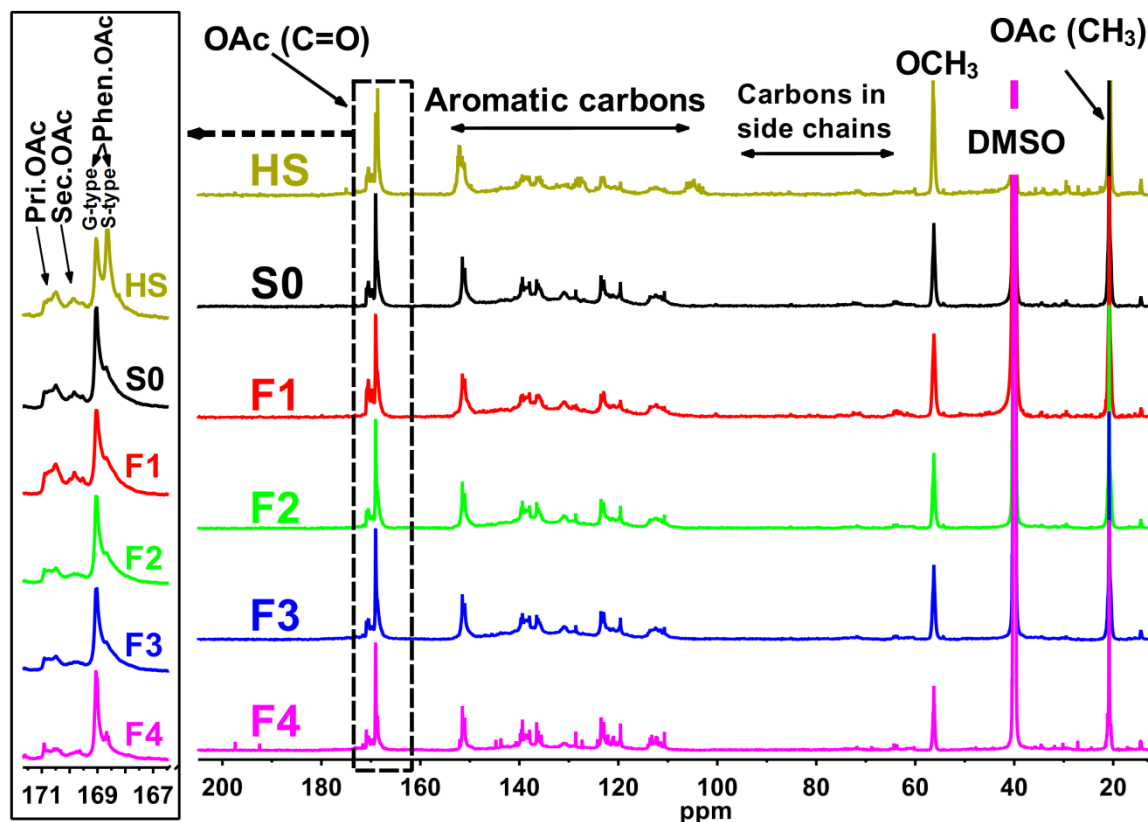

Figure 5.2 ^{13}C NMR spectra of lignin from softwood black liquor and its fractions and mixed hardwood/softwood black liquor.

^{1}H NMR

^{1}H NMR spectra of acetylated lignins are shown in Fig. 5.3, where acetylated aliphatic ($\delta_H \approx 2.1$ ppm) and phenolic ($\delta_H \approx 2.3$ ppm) hydroxyl and OMe ($\delta_H \approx 3.8$ ppm) groups are shown (Lundquist, 1991, 1992a, 1992b, Nagy *et al.*, 2010). It should be kept in mind that there is an overlap between aliphatic and phenolic hydroxyl groups in ^{1}H NMR spectra: therefore only the trend of the functional groups of lignin, rather than the absolute value, is in focus. The numbers of proton/aromatic rings ($\delta_H \approx 7$ ppm) are calibrated to 2.5 (Li and Lundquist, 1994) for kraft lignin, allowing the quantitative integration of acetylated hydroxyl and OMe groups to be calculated relative to this value.

A quantitative ^{1}H NMR evaluation (Table 5.2) suggests that, in the fractions containing smaller lignin molecules, the content of OH$_{phen.}$ is higher but the OH$_{ali.}$ is lower, whilst the content of OMe decreases as the MW of the lignin decreases, in agreement with the results obtained from ^{13}C NMR analysis.
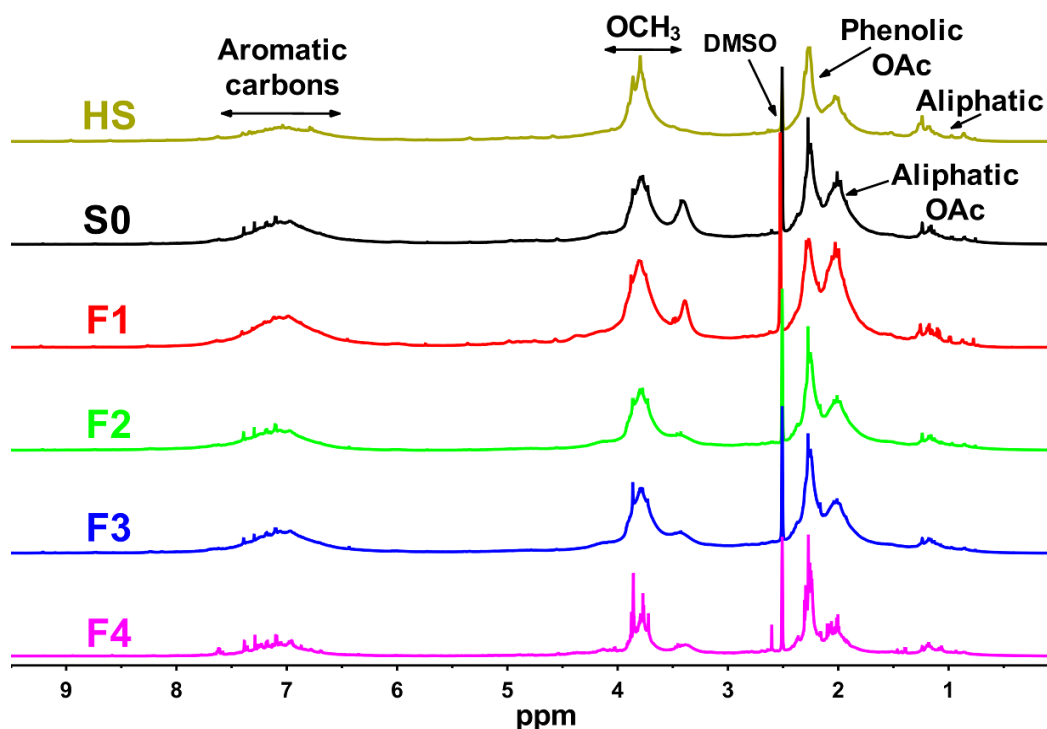
Figure 5.3 ^{1}H NMR spectra of lignin from softwood black liquor and its fractions and mixed hardwood/softwood black liquor.

5.1.3 Carbohydrates

The results reported in <u>Table 5.1</u> show that the concentration of carbohydrates in HS is higher than in S0: this is especially true for xylan, which is the major hemicellulose component of hardwood (Sjöström, 1993). It can also be found that the concentration of carbohydrates decreases from F1 to F4, along with a decrease in the MW of the lignin. This indicates that a majority of the carbohydrates is present together with lignin of a high MW, either as more or less "pure" carbohydrate molecules or as a lignin-carbohydrate complex (LCC). Moreover, the content of (galacto)glucomannan (GGM) seems to be lower than xylan in F1, F2 and F3. One possible explanation is that GGM is degraded more extensively than xylan during kraft pulping (Sjöström, 1993, Tenkanen *et al.*, 1999). These degraded GGM fragments present in the black liquor remain in the fraction with the lowest MWCO, so F4 therefore contains slightly greater amounts of GGM than xylan.

5.1.4 Other characteristics

The content of acid-soluble lignin (ASL) in HS shown in <u>Table 5.1</u> is quite high compared with that in S0. This is probably because HS consists of a high fraction of hardwood lignin which contains more ASL (Musha Y, 1974, Gellerstedt *et al.*, 2012). Moreover, it can also be seen that the fractions F2, F3 and F4 have much higher content of ASL than F1. This indicates that the ASL has a low MW, which is in agreement with a previous study by Yasuda *et al.*(2001).

The Na$_2$S content in F1 to F4 is found to be much lower than in the original S0, which is most likely due to the HS$^-$ being oxidized to S$_2$O$_3^{2-}$ (thiosulphate) during the fractionation of black liquor.

5.2 Precipitation yield of lignin in black liquor

5.2.1 Titration curves of BL (Papers I & III)

The buffer capacity of HS and S0 were studied in order to calculate the amount of hydrogen ions that are required to lower the pH of BL to a certain value. The titration curve for 1M HCl used is presented in Fig. 5.4. The result, *i.e.* the shapes of the plot curves, is that they are very similar to each other, which is in agreement with previous work (Wallmo *et al.*, 2009b). This indicates that the reaction of the different compounds in the two black liquors when acid is added is very similar. The curve can be divided roughly into three stages: neutralization of hydroxide ions (Region I), protonation of charged groups on the lignin molecule that make the lignin start to precipitate (Region II), and some buffering reactions (*e.g.* hydrogen sulphide and carbonate systems) (Wallmo *et al.*, 2007) in Region III. Naturally, these three stages overlap each other.
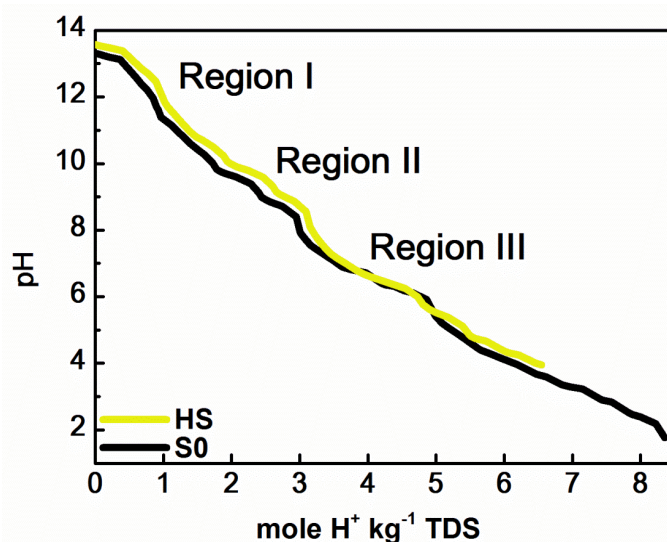

Figure 5.4 The buffer capacity curves of HS and S0.

5.2.2 Lignin precipitation of different BLs at various conditions (Papers I, III & IV)

In this work, the precipitation yield of lignin was calculated using the following equation:

$$Yield = \frac{L_{BL} - L_F}{L_{BL}} \times 100\% \tag{5.2}$$

where *Yield* is in percentage (%), L_{BL} is the lignin concentration of black liquor (g kg^{-1} TDS) before precipitation and L_F is the lignin concentration of the lignin-lean filtrate (g kg^{-1} TDS) obtained after precipitation. The lignin concentration was determined by applying the Klason lignin method.

5.2.2.1 Mixed hardwood/softwood BL (Paper I)

The precipitation yield of lignin from mixed HS at different pH, temperatures and additions of IS is shown in Fig. 5.5. As expected, it reveals that the highest yields are obtained at the lowest pH, because the increased protonation of the ionized phenolic groups on the lignin molecule neutralize its surface charges. The repulsive forces are reduced and

coagulation/precipitation of lignin occurs. In conclusion, a higher concentration of hydrogen ions (*i.e.* lower pH) will promote the protonation of phenolic groups and thus increase the precipitation yield of lignin.

Comparing the precipitation profiles at 45°C and 65°C in Fig. 5.5, it can be seen that the lignin yield decreases slightly with increasing temperature. This could be due to the electrostatic repulsive forces between the lignin molecules that increase with increasing temperature are also greater, and this may also favour the solubility of lignin. According to the DLVO theory (Shaw, 1993, Evans and Wennerström, 1999), if the repulsive forces dominate then the system will be more stable and, therefore, the solubility of lignin at higher temperature is higher. However, the attractive forces may also play a role in the stability of the system (Lee *et al.*, 2012), something that has not been considered in this case. Therefore, more investigation regarding this phenomenon will be investigated further in the future.

It is obvious from Fig. 5.5 that the lignin yield increases with increasing IS of the BL. The electrolytes may influence the system by means of the screening effect: increasing the IS reduces the range of repulsive interactions between the lignin molecules, which become close enough for attractive forces to become dominant.

It can be seen that, within the experimental conditions chosen, the precipitation pH has a stronger influence than the temperature and IS on the precipitation yield. However, it should be emphasized that the pH range from 9.5 to 11 corresponds to an increase in concentration of H^+ by approx. 30 times, which is much larger than the scale of changes caused by either temperature and IS.
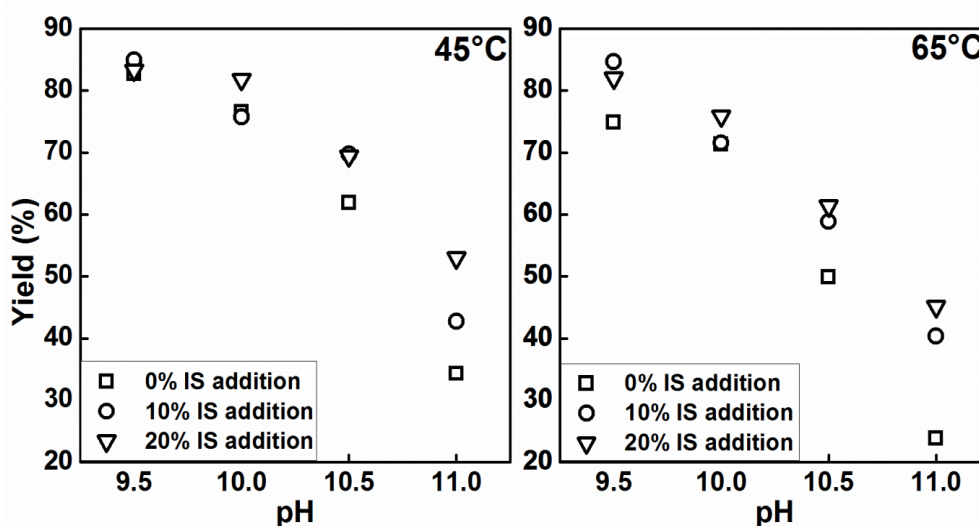

Figure 5.5 Precipitation yield of lignin from HS at various temperatures, pH and IS additions.

5.2.2.2 Softwood BL (Paper III)

The sum of the contents of sodium and potassium in the S0 was adjusted to be the same as in the HS, as mentioned earlier in Section 4.1. The precipitation yields of lignin from S0 are shown in Fig 5.6. In general, the trends of the yield from S0 at various conditions are the same as for HS. It is difficult, however, to compare the overall precipitation yield of lignin obtained

from these two black liquors because the differences in yield are small, often being close to the experimental error. Nevertheless, S0 shows a slightly higher precipitation yield of lignin than that of HS at the lowest/highest precipitation yield points. Two plausible reasons for this could be: 1) the MW of lignin in S0 is found to be higher than that in HS; NMR analysis also shows that the content of phenolic groups in softwood lignin is lower than in mixed hardwood/softwood lignin. This is in agreement with an earlier study by Norgren and Lindström (2000b), who found that kraft lignin with higher MW and a lower content of phenolic groups has a higher pK_a value. Therefore, a higher precipitation yield of lignin (*i.e.* lower solubility) from S0 is obtained; 2) both BLs has been adjusted to the same ionic strength (2.87 mole kg^{-1} liq.) but as S0 has a slightly higher concentration of lignin, this may influence the results to some extent (Öhman *et al.*, 2007c, Wallmo *et al.*, 2009a). In short, the differences in the highest/lowest precipitation yields obtained from the two BLs could be due to differences in the molecular structure (MW and phenolic group) of the lignin as well as slightly different concentrations of lignin in the BLs.
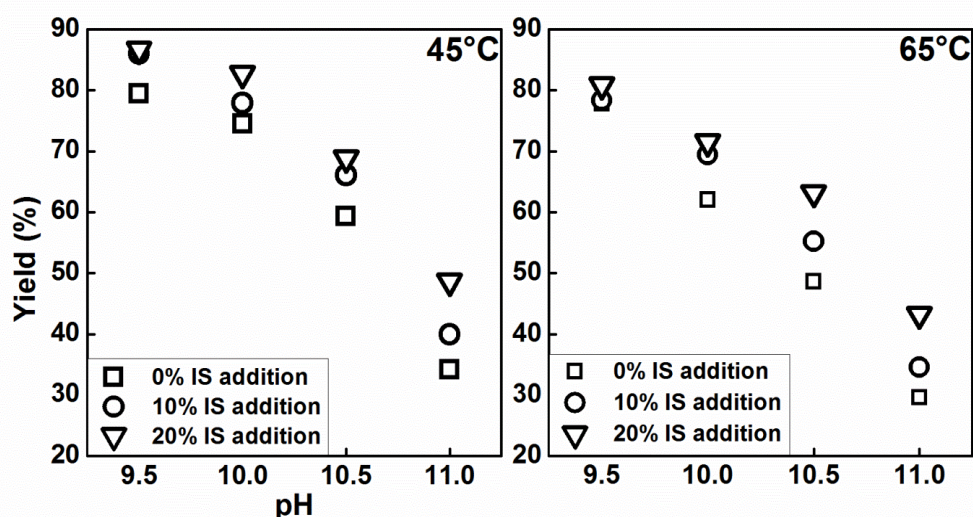

Figure 5.6 Precipitation yield of lignin from S0 at various temperatures, pH and IS additions.

5.2.2.3 Softwood BL fractions with different MWs (Paper IV)

The precipitation yield of lignin from fractions of S0 (F1, F2, F3 and F4) at various precipitation conditions is shown in Fig. 5.7. It shows that the precipitation yield follows the same trend as for HS and S0: that the yield increases with decreasing pH and/or temperature, or increasing IS. It is obvious from the figure that the precipitation yield of lignin differs significantly regarding MW: at the same conditions (*i.e.* the same pH, temperature and IS addition), the precipitation yield is: F1>F2>F3>F4. However, there is no big difference in the yield between F2 and F3, which is most likely due to the MW of the lignin between F2 and F3 being similar. The precipitation yield of each fraction is also compared with one reference case: the precipitation experiments using S0 at 65°C with no IS addition. It can be seen that the precipitation of lignin from F1 has a much higher yield than the reference, but the yields from F2, F3 and F4 are lower. One plausible explanation here could be that the largest lignin

molecules are expected to coagulate first, when the solution system is favourable for aggregation (Rudatin *et al.*, 1989, Norgren *et al.*, 2001).
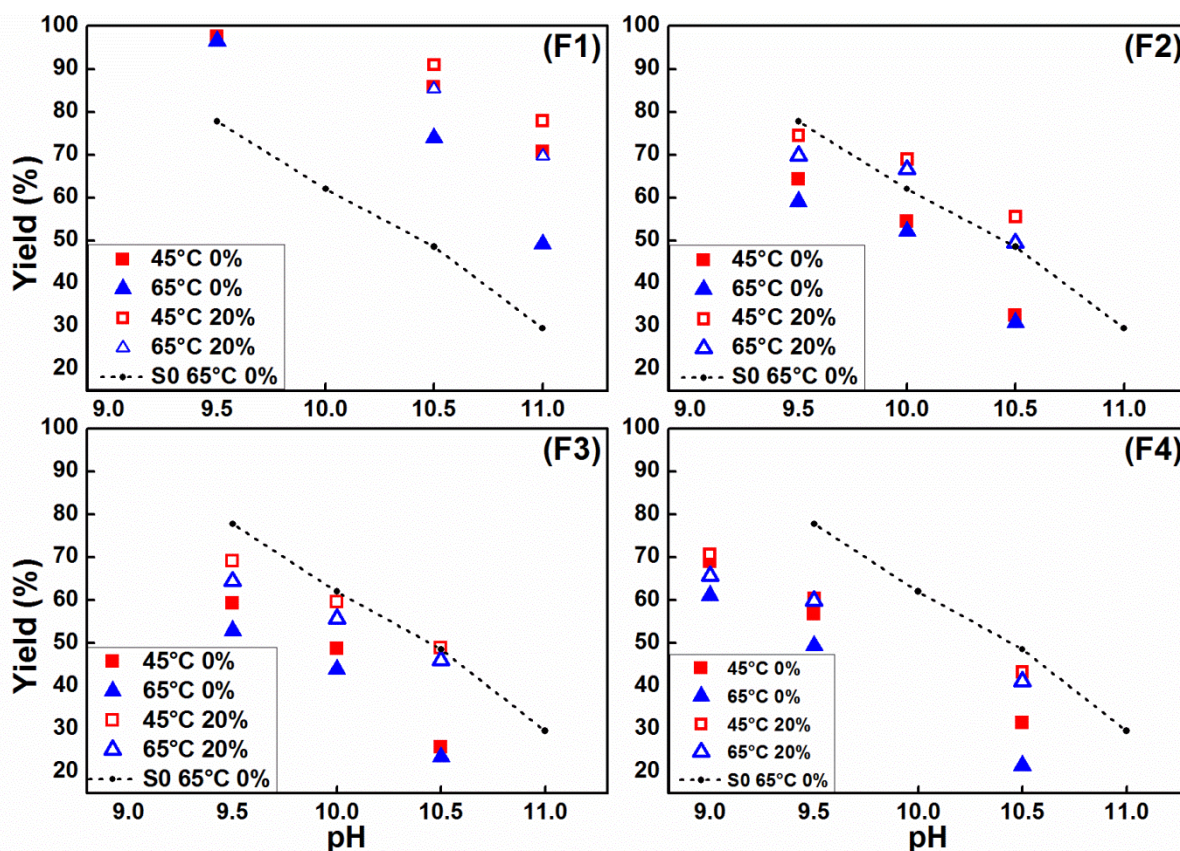

Figure 5.7 Precipitation yield of lignin from four S0 fractions at various conditions. The dotted line represents the yield curve of lignin from S0 at reference conditions.

5.2.3 The dissociation of phenolic groups on the lignin molecule in BL (Paper V)

5.2.3.1 Influences of precipitation conditions

The ratio of $\gamma_i(R_{cell})/\gamma_i(r)$ in Eq. 3.7 was assumed to be unity, as mentioned in Section 3.3. The approximation has been confirmed to be quite close to 1 (deviation $\leq 3.5\%$) after calculating this ratio using the Pitzer method and the PB cell programme (see Paper V). Consequently, it is an appropriate approximation and the dissociation degree (α) of phenolic groups on the lignin molecules in BL can be obtained by applying the classic Poisson-Boltzmann equation.

The estimated values of α calculated using the PB cell model (Section 3.3 and Appendix I) of different conditions for S0 are shown in Fig. 5.8.
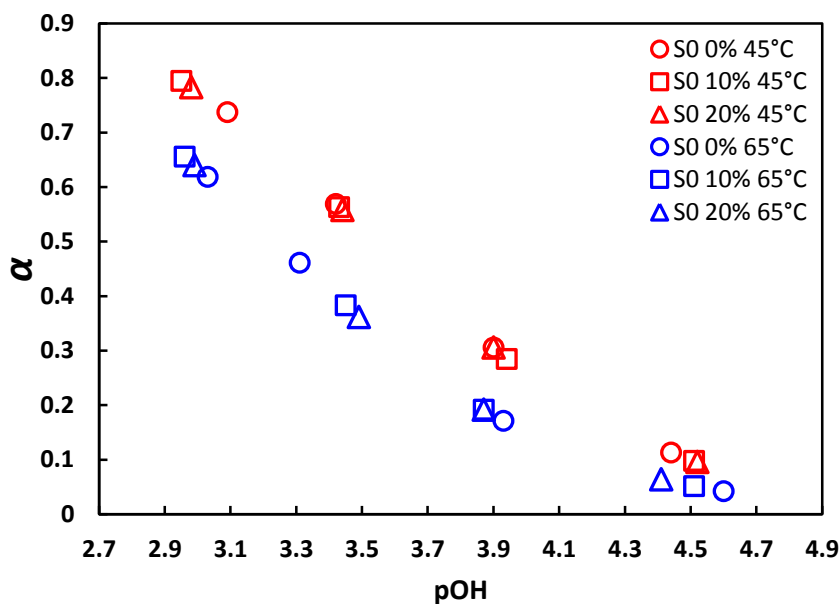
Figure 5.8 Predicted dissociation degree of phenolic groups on lignin (α profile) for S0 at different conditions. (0, 10 and 20% refer to the additions of the ionic strength of S0.)

As can be seen in Fig. 5.8, the value of α decreases with increasing pOH, *i.e.* the pH of the solution decreases, which indicates that the reverse reaction of lignin dissociation (protonation) is dominant. This can be explained by the higher concentration of H^+ in the system (due to the decrease in pH), which allowed the lignin phenolate ($L–O^-$) to protonate to a higher degree.

Fig. 5.8 shows that the α values calculated at 45°C are higher than those at 65°C, indicating that the dissociation degree of the phenolic groups on the lignin decreased as the temperature increased. This prediction is in agreement with previous studies (Norgren and Lindström, 2000a, Norgren *et al.*, 2001) and can be explained using the Van 't Hoff equation (Eq. 3.12): whilst the K_a value of kraft lignin increases as the temperature increases, the ionic product of water (K_w) increases even more than the K_a of lignin (Norgren, 2001), *i.e.* $\frac{K_a}{K_w} < 1$. Assuming that $\{H^+_{surf.}\} \approx \{H^+_{bulk}\}$ and combining Eq. 3.11 with the dissociation equation of water allows Eq. 5.3 to be obtained:

$$\frac{K_a}{K_w}\{OH^-_{bulk}\} = \frac{1}{\frac{1}{\alpha}-1} \tag{5.3}$$

where $\{OH^-_{bulk}\}$ is the activity of hydroxide ions in the solution, and can be considered independent of the temperature-induced changes in the dissociation of water (Norgren and Lindström, 2000a). With increasing temperature, the left side in Eq. 5.3 decreases (as discussed above) and, consequently, α also decreases. A lower α value indicates a higher degree of protonation. At first glance, however, this result is unexpected because, according to the experimental results, the precipitation yield increases with decreasing temperature. It should be kept in mind that, prior to precipitation, the lignin has firstly been protonated and thereafter "coagulated". Consequently, it may be a phenomenon related to the latter process

that strongly promotes coagulation when the temperature decreases (see also Section 5.2.2.1). The reasoning will be investigated further in the future.

The α values for different IS additions seem to follow almost the same curve for a given temperature (Fig. 5.8). The sum of the sodium and potassium contents in S0 is quite high (Table 5.1), so the lignin macromolecules are already strongly screened in black liquor, *i.e.* the cations have organized themselves around the surface of lignin molecules to minimize the electric fields (Shaw, 1993). Therefore a slight increase in IS has no or little effect on the dissociation of the phenolic groups on lignin molecules in such highly concentrated electrolyte solutions.

Fig 5.9 shows that, for the lignin fractions F1, F2 and F4, there are distinct differences in their MW while their corresponding dissociation curves are independent on the molecular size for a given pOH and temperature. The insensitivity to MW in the prediction of α is due to the differences in the electrostatic potential obtained by varying the size of the lignin within the range relevant in this study, which result in insignificant variations in the predicted pH and, consequently, α. This is apparent when $\Delta[H^+] \propto e^{\Delta\Phi}$ and the small absolute values of $\Delta\Phi$ are considered (where Δ refers to the difference between two different molecular weights/sizes).
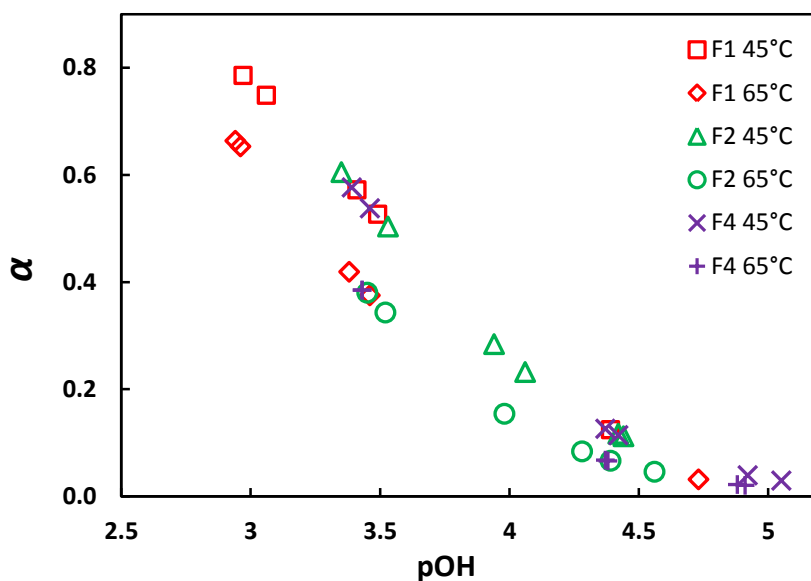

Figure 5.9 Dissociation degree of phenolic groups on lignin for the lignin fraction with different MWs.

5.2.3.2 Relationship between α and the precipitation yield

The precipitation yield of lignin increased, in general, with decreasing α, as can be seen in Fig. 5.10, indicating that more lignin molecules are protonated and that precipitation is favoured. Moreover, lignin precipitated in the S0 at 45°C shows a higher yield compared with 65°C: this was also observed in previous studies of HS (Section 5.2.2.1) and discussed in Section 5.2.3.1. On the other hand, the BL fraction with the largest lignin molecules (F1) seems to achieve the highest precipitation yield at the same α value. This observation indicates that

lignin with a high MW tends to aggregate/coagulate to a higher extent than those with a low MW, which is in agreement with the discussion in Section 5.2.2.3.
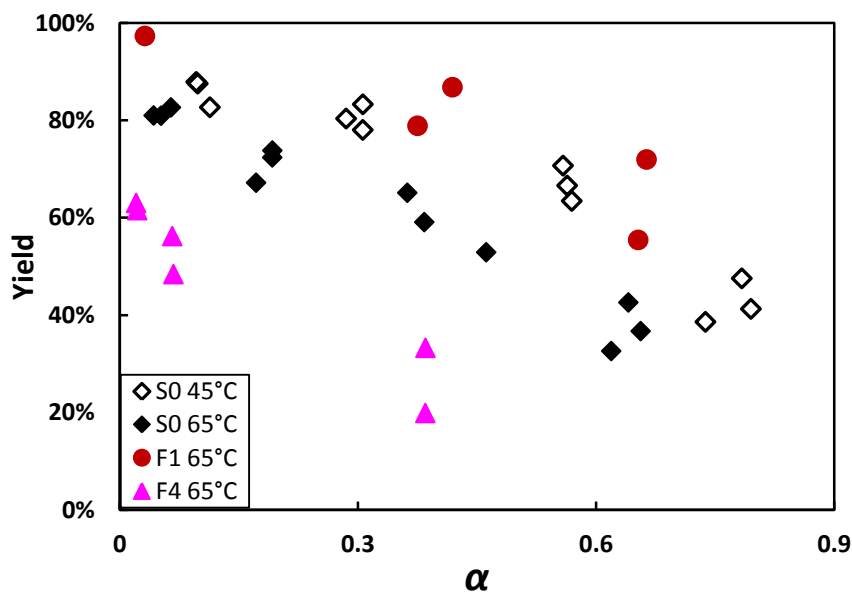

Figure 5.10 The precipitation yield of lignin from S0 at various degrees of dissociation of its phenolic groups.

5.3 Characterization of precipitated lignin

5.3.1 Molecular weight of precipitated lignin (Papers I - IV)

5.3.1.1 M_w vs. precipitation yield (Paper II)

The relationship between the precipitation yield and the weight-average molecular weight (M_w) of the lignin precipitated from HS under different conditions is shown in Fig. 5.11.
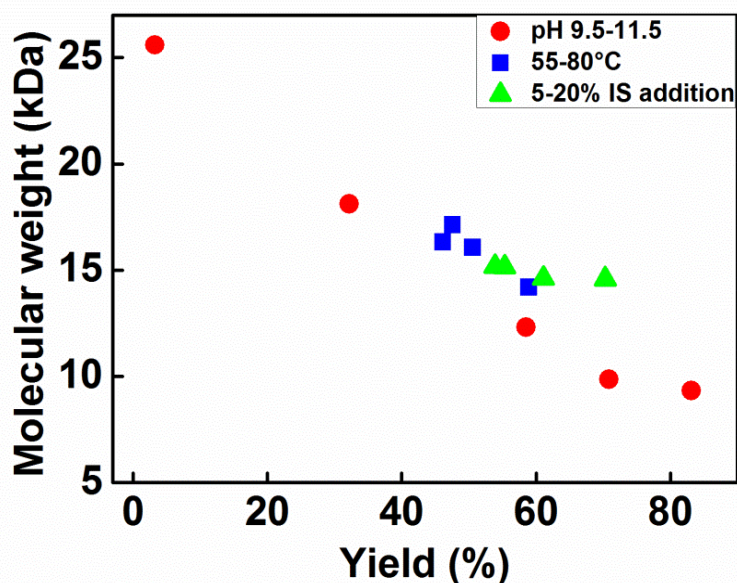

Figure 5.11 The weight-average molecular weight of lignin (UV detector) precipitated from HS at different yield levels.

It can be seen that the M_w of lignin decreases with increasing precipitation yield, which indicates that there is an increasing amount of lignin of lower MW that is being precipitated at a high precipitation yield. This is in agreement with the previous discussion in Section 5.2.2.3 that larger lignin molecules precipitate at higher pH (low yield). As the solution's condition is getting worse (by decreasing the pH), smaller lignin molecules start to precipitate and thus increase the total precipitation yield, while the overall MW of the precipitated lignin decreases. It can be noted that there is a good general correlation between the MW and the process conditions investigated; although both the pH and temperature seem to have a similar effect on the changes in the MW of the lignin, IS shows a smaller effect. This suggests that, within the experimental conditions chosen, the pH and temperature are the main parameters that determine the MW of precipitated lignin.

5.3.1.2 Mixed hardwood/softwood black liquor vs. softwood black liquor (Papers I & III)

The differences in M_w between the lignins precipitated from HS and S0 are reported in Table 5.3. It shows that the M_w value measured by RI response was higher than that measured using UV response, which is mainly due to the RI detector having a lower sensitivity than the UV detector in the region of lower MWs, and the fact that the MW fraction below the detection limit of RI being omitted (Figs. 5.1 and 5.12). However, within the same precipitation conditions, the lignin obtained from S0 has a higher M_w than that from HS. This is in agreement with previous discussion in Section 5.1.1.

**Table 5.3** Comparison of the weight-average molecular weight of the lignin precipitated from HS and S0.

Sample №.	IS addition (%)	Precipitation pH	T (°C)	M_w (kDa)				Yield (%)	
				HS		S0		HS	S0
				RI	UV	RI	UV		
1	20	9.5	45	10.8	8.8	16.7	14.5	83.3	86.7
2	10	10	65	13.5	10.9	17.7	15.2	71.6	69.5
3	0	11	75	15.3	13.1	26.9	24.9	22.0	26.4
4	0	9.5	65	13.4	10.3	17.3	15.0	74.9	77.8
5	0	10	65	14.5	11.7	18.1	15.2	71.4	62.0
6	0	10.5	65	15.0	12.3	18.3	15.4	49.9	48.6
7	0	11	65	15.2	12.5	19.7	16.2	23.8	29.6

5.3.1.3 Softwood black liquor fractions

Fig. 5.12 illustrates the molecular weight distribution (MWD) of the lignin precipitated from the fractions (*i.e.* F1, F2, F3 and F4) with the highest/lowest precipitation yield (given in Table 5.4). It can be seen that the distribution curves of F1 and F4 are well separated but those of F2 and F3 are rather similar. Furthermore, lignin with a very high MW (>100 kDa) in F1 was precipitated at high pH.

Table 5.4 Precipitation conditions and yield of lignin obtained from each black liquor fraction.

Sample name	pH	Temperature (°C)	IS addition (%)	Yield (%)
F1 high yield	9.5	45	0	97.5
F1 low yield	11	65	0	49.2
F2 high yield	9.5	45	20	74.5
F2 low yield	10.5	65	0	31.0
F3 high yield	9.5	45	20	69.1
F3 low yield	10.5	65	0	23.5
F4 high yield	9	45	20	70.7
F4 low yield	10.5	65	0	21.5
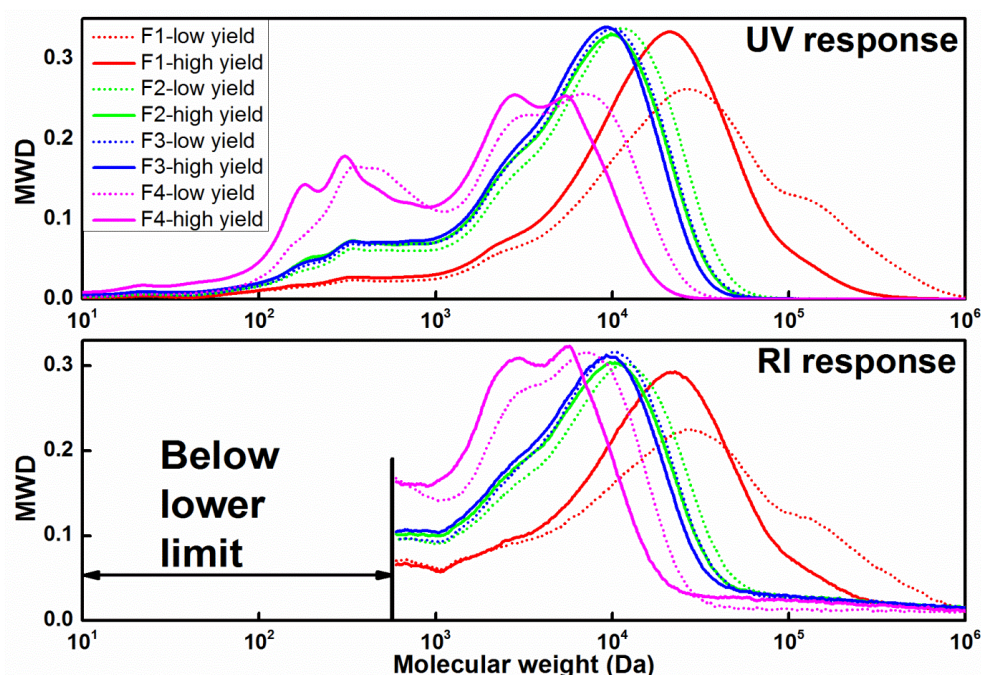
Figure 5.12. Molecular weight distribution (MWD) of the lignin precipitated with the highest/lowest yields from the softwood black liquor fractions.

5.3.2 Functional groups (Papers I, II & III)

5.3.2.1 Mixed hardwood/softwood black (Paper II)

Some of the precipitation conditions for the HS used are presented in Table 5.5 along with the results from ^{13}C NMR spectra of acetylated lignin precipitated; some of the spectra of the samples are given in Fig. 5.13. As can be seen in Table 5.5, the amount of $OH_{phen.}$ increases from Sample 1 to 5 as the precipitation yield increases. The trend of a higher $OH_{phen.}$ content at a higher yield can be explained by the fact that more lignins with low MWs are precipitated at higher precipitation yields, as shown in Fig. 5.11. These small lignin molecules have more $OH_{phen.}$ groups due to the split β-O-4 linkages (Gellerstedt and Lindfors, 1984, Gellerstedt, 2009).
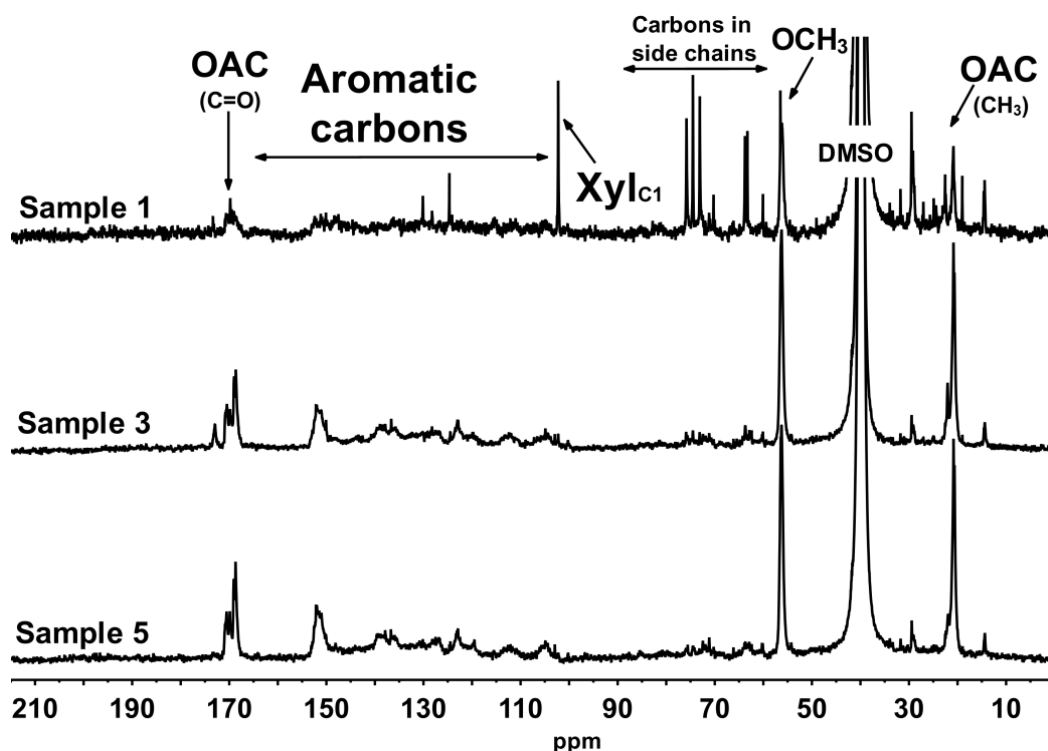
Figure 5.13 ^{13}C NMR spectra of the lignin precipitated from mixed hardwood/softwood kraft black liquor.

Table 5.5 shows that the amount of OMe groups seems to increase from Samples 1 to 5, *i.e.* in the order of increasing precipitation yield (decreasing MW of the precipitated lignin). In this study, the S/G ratio was determined according to earlier investigations (Mörck *et al.*, 1988, Pu and Ragauskas, 2005, Samuel *et al.*, 2010) based on the peaks in the regions δ_C 102–109 and 110–121 ppm, which represent C_2/C_6 in the syringyl and guaiacyl units in the precipitated lignin. In agreement with the literature, the S/G ratios of precipitated lignin with lower MWs are greater than those with higher MWs (Mörck *et al.*, 1988, Toledano *et al.*, 2010b).

The xylan signal (Xyl_{C1}) in the ^{13}C NMR spectra is also given in Table 5.5. The results show that the lignin precipitated at a higher pH has a higher MW and a higher xylan content.

Table 5.5 Quantitative comparison of mixed hardwood/softwood kraft lignin, precipitated at various pH levels at 45°C and with no IS addition, based on ^{13}C NMR spectra. (All values are calculated on a 100 C_9 basis.)

Sample №.	pH	Yield (%)	M_w (UV) kDa	Ac.OH$_{phen.}$ 166–269.5 ppm	OMe 54–57.5 ppm	Xyl$_{C1}$ 100–102 ppm	S/G ratio
1	11.5	3.2	25.6	36	97	23	0.49
2	11	32.1	18.1	60	146	11	0.50
3	10.5	58.5	12.3	62	149	5	0.53
4	10	70.9	9.9	65	153	3	0.54
5	9.5	83.1	9.3	66	155	1	0.60

5.3.2.2 Comparison of mixed hardwood/softwood and softwood kraft lignin (Papers I & III)

The NMR results for lignin precipitated from S0 and HS are reported in Table 5.6, where the same trend regarding the phenolic groups can be discerned. However, the overall concentration of phenolic groups on the lignin precipitated from the HS is higher than that from S0. A possible explanation for this could be that the lignin in the HS has a lower MW: hardwood lignin is degraded more heavily during cooking and thus contains more free phenolic groups (see also Section 5.1.2). The content of the OMe group is found to be higher in mixed lignin than in softwood lignin, which is due to the S-type of lignin present in hardwood. Another finding is that, in the precipitated softwood kraft lignin, the content of the OMe group increases as the MW of the lignin increases. On the other hand, the content of the OMe group decreases when the MW of mixed hardwood/softwood lignin increases: this could be due to the precipitated lignin with a low MW containing more S-type lignin, whereas precipitated lignin with a high MW contains more G-type lignin.

Table 5.6 Quantitative comparison of mixed hardwood/softwood and softwood kraft lignin based on ^{13}C NMR spectra. (All values are calculated on a 100 C_9 basis.)

Sample №.[*]	Ac. OH$_{phen.}$ 166–169.5 ppm		OMe 54–57.5 ppm	
	HS	S0	HS	S0
1	120	89	162	70
2	102	86	150	74
3	84	80	138	79
4	108	87	156	72
5	102	85	150	75
6	96	83	150	77
7	96	81	156	78

*The same sample series given in Table 5.3.

5.3.3 Carbohydrates (Papers II & III)

Table 5.7 Concentrations (g kg^{-1} TDS) of xylan and (galacto)glucomannan (GGM) in the kraft lignin precipitated from black liquor samples with various additions of IS.

IS addition (%)	Carbohydrates	Concentrations (g kg^{-1} TDS)	
		HS	S0
0	Xylan	18.7 ± 6.6	6.3 ± 0.7
	GGM	3.1 ± 0.8	7.0 ± 2.5
10	Xylan	26.5 ± 8.0	7.0 ± 0.5
	GGM	5.1 ± 2.2	7.4 ± 2.4
20	Xylan	29.1 ± 11.3	7.2 ± 0.8
	GGM	5.6 ± 1.9	7.2 ± 2.5

The concentrations of xylan and GGM in lignin precipitated from HS and S0 at different levels of IS additions are given in Table 5.7. It can be seen that the amount of xylan is higher, and the GGM content is lower, in the lignin precipitated from HS compared with that from S0. One possible explanation here is that hardwood contains more xylan than softwood, and GGM is the dominate hemicellulose in softwood (Sjöström, 1993, Henriksson *et al.*, 2009).

Table 5.8 Concentrations of xylan and GGM (g kg^{-1} TDS) in softwood kraft lignin precipitated at various pH and temperatures.

	Concentrations of carbohydrates (g kg^{-1} TDS)							
	45 (°C)				65 (°C)			
pH	9.5	10	10.5	11	9.5	10	10.5	11
Xylan	5.9 ± 0.6	6.6 ± 0.7	6.8 ± 0.9	7.8 ± 0.7	6.6 ± 0.2	6.7 ± 0.3	6.6 ± 0.5	6.7 ± 0.6
GGM	3.1 ± 0.4	4.9 ± 1.0	6.5 ± 0.5	9.7 ± 0.4	7.3 ± 0.3	7.5 ± 0.3	8.5 ± 0.2	10.7 ± 0.5

The concentrations of xylan and GGM in the lignin precipitated from S0 are listed in Table 5.8. It can be seen that, at 45°C and a pH range between 9.5 and 11, the concentration of xylan increased with increasing pH (*i.e.* a lower yield). As discussed earlier (Section 5.3.1.2), the precipitated lignin had a higher MW at higher pH levels. One possible reason is that larger LCC molecules that precipitate at a high pH have a higher content of carbohydrates, since it is likely that they have been degraded to a lesser degree during kraft cooking.

The same trend was also found for GGM in the lignin precipitated at 45°C, but the increase was greater than that of xylan. A plausible reason for this might be that the lignin precipitated at a lower pH has a lower MW: this indicates heavier degradation which, in turn, would result in a lesser amount of GGM being left in the LCC structure. At 65°C, the concentration of GGM increased with increasing precipitation pH, while that of xylan seems to be independent of pH. Another observation is that the overall GGM content was much higher at 65°C compared with 45°C, especially at pH levels of 9.5 and 10. This is in agreement with the discussion above: at lower temperatures (higher yields), lignin molecules of low MW are also precipitated, so the lignin that is precipitated therefore contains lesser amounts of GGM. It has also been suggested by Lawoko *et al.* (2005) that, during cooking, GGM-linked lignin undergoes a partial condensation that causes larger molecules to be formed. This is in agreement with the observations made here, *i.e.* the content of GGM in the precipitated lignin is increases with increasing MW.

The concentrations of xylan and GGM in the lignin precipitated from HS are shown in Figure 5.14. The trend for the carbohydrate content when the temperature is increased, seems to behave differently compared to softwood kraft lignin. For example, it can be seen that, at a constant pH of 10.5, the concentration of xylan decreases as the temperature increases. Although the reason for this is not fully understood yet, one possible explanation for this could be that the pK_a of xylan (mainly the carboxylic groups, where p$K_a \approx 4.4$ (Öhman and Theliander, 2006)) is lower than the pK_a of "pure" lignin. The LCC with a low xylan content

will thus have a higher effective pK_a than the LCC with a higher xylan content. On the other hand, the pK_a of lignin decreases as the temperature increases and the lignin becomes more soluble: therefore only the lignin with lesser contents of xylan could be precipitated at higher temperatures.

The concentration of GGM seems to be independent of temperature, which could be due to the fact that the smaller lignin molecules have been degraded intensively during cooking and only a trace amount of GGM is bonded to the kraft lignin.
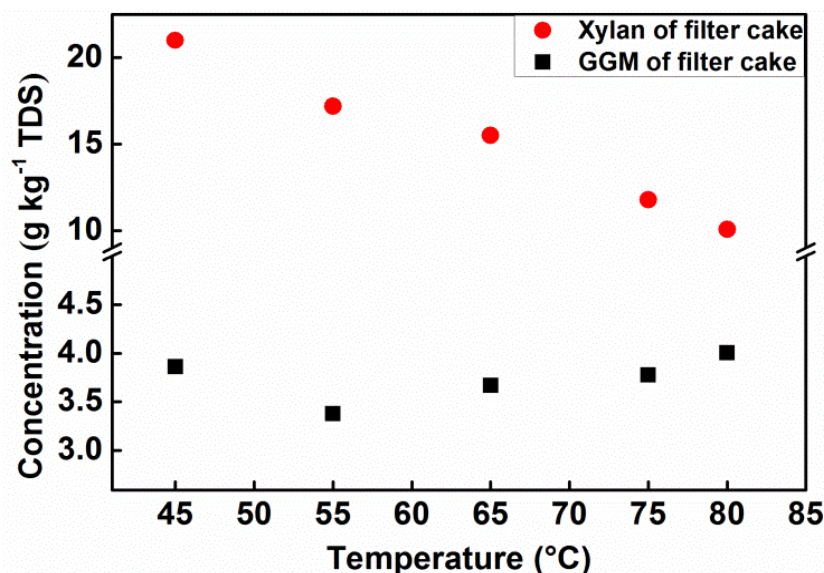
Figure 5.14 Concentrations of xylan and GGM in the lignin precipitated from HS at pH 10.5.

6. CONCLUDING REMARKS

1) The precipitation yield of lignin from BL increases with decreasing pH/temperature and/or increasing ionic strength of BL.

2) The amount lignin with a lower MW increases as the precipitation yield increases.

3) Overall, softwood black liquor and mixed hardwood/softwood black liquor have similar precipitation yields of lignin. Softwood black liquor, however, seems to have a higher yield for the corresponding highest/lowest precipitation yield compared with the mixed hardwood/softwood black liquor used in this study.

4) Membrane filtration is a feasible method for obtaining more homogeneous lignin fractions in BL. Moreover, within the same precipitation conditions, the lignin fraction with the highest MW tends to give the highest precipitation yield.

5) According to NMR analysis, the content of phenolic groups in kraft lignin is found to increase as the precipitation yield increases; the mixed hardwood/softwood kraft lignin has a higher content of phenolic groups than the softwood kraft lignin.
The kraft lignin precipitated from the mixed BL has a higher content of OMe groups than the softwood kraft lignin. The content of OMe in the lignin precipitated from the mixed BL increases as the yield increases whilst it decreases with increasing yield in the lignin from softwood BL.

6) The content of carbohydrates (most likely in the form of LCC) in the precipitated lignin decreases as the yield increases; it is higher at higher temperatures in lignin from unfractionated softwood BL. It is also found that the kraft lignin precipitated from mixed hardwood/softwood BL contains a higher amount of carbohydrates than that from softwood kraft lignin.

7) The dissociation degree of phenolic groups on lignin, α, is obviously related to the pOH (pH) and temperature in the precipitation step. In the black liquor system, increasing the IS of BL seems to have no/little effect on the dissociation of phenolic groups, which indicates the highly screened condition of the BL system. Moreover, the precipitation yield is related not only to the value of α but also to the balance of attractive and repulsive forces between the lignin macromolecules, which influences the yield of lignin precipitation.

7. FUTURE WORK

This study has investigated the apparent equilibrium of lignin precipitation in black liquor from two different perspectives: process conditions and molecular properties of lignin. In the black liquor system, the protonation of phenolic groups on lignin seems to be related to the pH and temperature prevalent during precipitation. However, both the ionic strength of the BL and the molecular properties of lignin influence its precipitation yield. The following are suggestions of topics that may be of interest to investigate in the future:

1) The manner in which protonated lignin molecules start to aggregate together and continue to grow into a larger agglomerate. The DLVO theory plays an important part in considering the total balance between the repulsive and attractive forces between the lignin molecules in a black liquor system.

2) A further study of the kinetics of the growth of particles on lignin molecules in black liquor at various precipitation conditions. This would provide a more detailed picture of the precipitation of lignin in black liquor.

3) A comparative investigation in which the ionic strength of the black liquor is lowered drastically to study if changing the ionic strength (in the low electrolyte system) influences the dissociation degree of the phenolic groups on lignin. Whether or not lignin molecules of different MWs have different dissociation curves in the low electrolyte system could also be studied.

4) A 2D-NMR analysis could be performed to investigate the structure of the precipitated lignin in more details with respect to the different linkages between a) lignin units and b) lignin units and carbohydrates.

8. NOMENCLATURE

BL   Black liquor

HS   Mixed hardwood/softwood black liquor

S0   Unfractionated softwood black liquor

F1   Fractionated softwood black liquor: Fraction 1

F2   Fractionated softwood black liquor: Fraction 2

F3   Fractionated softwood black liquor: Fraction 3

F4   Fractionated softwood black liquor: Fraction 4

AAS   Atomic absorption spectroscopy

Ac   Acetyl

ASL   Acid-soluble lignin

DMSO   Dimethyl sulphoxide

G   Guaiacyl

GGM   (Galacto)glucomannans

GPC   Gel permeation chromatography

HPAEC-PAD   High-performance anion exchange chromatography with pulsed
                amperometric detection

HPLC   High performance liquid chromatography

IC   Ion chromatography

IS   Ionic strength

LCC   Lignin-carbohydrates complex

M_n Number-average molecular weight

M_w Weight-average molecular weight

MW   Molecular weight

MWCO   Molecular weight cut-off

MWD   Molecular weight distribution

NMR   Nuclear magnetic resonance

OAc   Acetoxyl group

OMe   Methoxyl group

PB	Poisson-Boltzmann
PD	Polydispersity
RI	Refractive index
S	Syringyl
TDS	Total dry solid
VR	Volume reduction
VRF	Volume reduction factor

F	Faradays constant (C mole^{-1})
K_a	Dissociation constant of phenolic group on lignin molecules (mole m^{-3})
K_w	Ionization constant of water (mole m^{-3})
L_{BL}	Lignin concentration in black liquor (g kg^{-1} TDS)
L_L	Lignin concentration in filtrate (g kg^{-1} TDS)
pK_a	Logarithmic constant of K_a

R_{cell}	Radius of the cell in PB-cell model (Å)
$R_{lig.}$	Radius of the lignin in PB-cell model (Å)
c_i	Concentration of electrolyte, i, (mole m^{-3})
z_i	Valence number of electrolyte, i, (-)
α	Dissociation degree of phenolic group on lignin molecules (-)
γ	Activity coefficient (-)
ε_0	Permittivity in vacuum (F m^{-1})
ε_r	Relative permittivity of the liquid (F m^{-1})
ρ	Volumetric charge density (C m^{-3})
σ_0	Surface charge density of total dissociated phenolic groups on lignin (C m^{-2})
Φ	Electrostatic potential (V)
ΔH	Constant dissociation enthalpy (kJ mole^{-1})

9. ACKNOWLEDGEMENTS

10. BIBLIOGRAPHY

Adler, E. 1977. Lignin chemistry—past, present and future. *Wood Science and Technology,* 11**,** 169-218.

Alén, R., Patja, P. & Sjöstrom, E. 1979. Carbon dioxide precipitation of lignin from pine kraft black liquor *Tappi,* 62**,** 108-110.

Alén, R., Sjöström, E. & Vaskikari, P. 1985. Carbon dioxide precipitation of lignin from alkaline pulping liquors. *Cellulose Chemistry and Technology,* 19**,** 537-541.

Arkell, A., Olsson, J. & Wallberg, O. 2014. Process performance in lignin separation from softwood black liquor by membrane filtration. *Chemical Engineering Research and Design,* 92**,** 1792-1800.

Bozell, J., Holladay, E., Johnson, D. & White, J. F. 2007. Top value added chemicals from biomass. Volume II – results of screening for potential candidates from biorefinery lignin. Richland, WA, USA: Pacific Northwest national laboratory and national renewable energy laboratory.

Chakar, F. S. & Ragauskas, A. J. 2004. Review of current and future softwood kraft lignin process chemistry. *Industrial Crops and Products,* 20**,** 131-141.

Choi, J. W. & Faix, O. 2011. NMR study on residual lignins isolated from chemical pulps of beech wood by enzymatic hydrolysis. *Journal of Industrial and Engineering Chemistry,* 17**,** 25-28.

Clay, D. T. 2011. Evaporation principles and black liquor properties. Available: http://www.tappi.org/content/events/08kros/manuscripts/3-1.pdf.

Connors, W. J., Sarkanen, S. & Mccarthy, J. L. 1980. Gel chromatography and association complexes of lignin. *Holzforschung,* 34**,** 80.

Delville, A. 1984. Interactions between ions and polyelectrolytes: A note on determination of ionic activities, with reference to a modified Poisson-Boltzmann treatment. *Biophysical Chemistry,* 19**,** 183-189.

Dence, C. W. 1992. The determination of lignin. *In:* Lin, S. & Dence, C. W. (eds.) *Methods in Lignin Chemistry* Heidelberg, Germany: Springer-Verlag.

Deserno, M. & Holm, C. 2001. Cell model and Poisson-Boltzmann theory: a brief introduction. *In:* Holm, C., Kékicheff, P. & Podgornik, R. (eds.) *Electrostatic effects in soft matter and biophysics.* Springer Netherlands.

Donald, D. 2010. Overview. *In:* Heitner, C., Dimmel, D. R. & Schmidt, J. A. (eds.) *Lignin and Lignans: Advances in Chemistry.* Boca Raton, USA: CRC Press.

Eriksson, Ö., Goring, D. a. I. & Lindgren, B. O. 1980. Structural studies on the chemical bonds between lignins and carbohydrates in spruce wood. *Wood Science and Technology,* 14**,** 267-279.

Evans, D. F. & Wennerström, H. 1999. Colloidal stability. *In:* Evans, D. F. & Wennerström, H. (eds.) *The colloidal domain: where physics, chemistry, biology, and technology meet.* 2nd Ed. Danvers, MA, USA: Wiley-VCH

Faix, O., Argyropoulos, D. S., Robert, D. & Neirinck, V. 1994. Determination of hydroxyl groups in lignins evaluation of ^{1}H-, ^{13}C-, ^{31}P-NMR, FTIR and wet chemical methods. *Holzforschung,* 48**,** 387-394.

Finaldi, L. 2013. *Domtar unveils new technology at Plymouth facility* [Online]. www. newsobserver.com. Available: http://www.newsobserver.com/2013/06/08/2946499/domtar-unveils-new-technology.html.

Frederick, W. J. 1997. Black liquor properties. *In:* Adams, T. N. (ed.) *Kraft recovery boilers.* Atlanta, GA, USA: Tappi Press.

Froass, P. M., Ragauskas, A. J. & Jiang, J. E. 1998. NMR studies Part 3: analysis of lignins from modern kraft pulping technologies. *Holzforschung,* 52**,** 385-390.

Gellerstedt, G. 2009. Chemistry of chemical pulping. *In:* Ek, M., Gellerstedt, G. & Henriksson, G. (eds.) *The Pulp and Paper Chemistry and Technology, Volume 2 Pulping Chemistry and Technology.* Berlin, Germany: De Gruyter.

Gellerstedt, G. & Henriksson, G. 2008. Lignins: major sources, structure and properties. *In:* Mohamed, B. & Alessandro, G. (eds.) *Monomers, Polymers and Composites from Renewable Resources.* Amsterdam, The Netherlands: Elsevier.

Gellerstedt, G. & Lindfors, E.-L. 1984. Structural changes in lignin during kraft pulping. *Holzforschung,* 38**,** 151-158.

Gellerstedt, G., Sjöholm, E. & Brodin, I. 2010. The wood-based biorefinery: a source of carbon fiber? *Open Agriculture Journal,* 4**,** 119-124.

Gellerstedt, G., Tomani, P., Axegård, P. & Backlund, B. 2012. Lignin recovery and lignin-based products. *In:* Lew, C. (ed.) *Integrated Forest Biorefineries: challenges and opportunities.* Cambridge, UK: Royal Society of Chemistry.

Gierer, J. 1970. The reactions of lignin during pulping. A description and comparison of conventional pulping processes. *Svensk Papperstidning,* 73**,** 571-596.

Gierer, J. 1980. Chemical aspects of kraft pulping. *Wood Science and Technology,* 14**,** 241-266.

Goring, D. a. I. 1962. The physical chemistry of lignin. *Pure and Applied Chemistry,* 5**,** 233-310.

Goring, D. a. I. 1971. Polymer properties of lignin and lignin derivatives. *In:* Sarkanen, K. V. & Ludwig, C. H. (eds.) *Lignins: occurrence, formation, structure and reactions.*

Gullichsen, J. 1999. Fiber line operations. *In:* Gullichsen, J. & Fogelholm, C.-J. (eds.) *Chemical pulping.* Helsinki, Finland: Fapet Oy.

Gunnarsson, G., Joensson, B. & Wennerstroem, H. 1980. Surfactant association into micelles. An electrostatic approach. *The Journal of Physical Chemistry,* 84**,** 3114-3121.

Henriksson, G., Brännvall, E. & Lennholm, H. 2009. The trees. *In:* Ek, M., Gellerstedt, G. & Henriksson, G. (eds.) *The Pulp and Paper Chemistry and Technology, Volume 1 Wood Chemistry and Wood Biotechnology.* Berlin, Germany: De Gruyter.

Higson, A. 2011. Lignin. Factsheet: overview of the current and potential market for lignin based materials. www.nnfcc.co.uk.

Holmqvist, A., Wallberg, O. & Jönsson, A. S. 2005. Ultrafiltration of kraft black liquor from two Swedish pulp mills. *Chemical Engineering Research and Design,* 83**,** 994-999.

Hough, W. J. 1910. *Process of treationg spent alkaline pulping liquors.* USA patent 432932.

Innventia. 2007. *Lignoboost demonstration plant* [Online]. INNVENTIA. Available: http://www.innventia.com/en/Our-Ways-of-Working/Demonstration-and-pilot/Lignoboost-demonstration-plant-/.

Janson, J. 1974. Analysis of the polysaccharides in wood and pulp. *Faserforschung und Textiltechnik,* 25**,** 375-382.

Jönsson, A.-S., Nordin, A.-K. & Wallberg, O. 2008. Concentration and purification of lignin in hardwood kraft pulping liquor by ultrafiltration and nanofiltration. *Chemical Engineering Research and Design,* 86**,** 1271-1280.

Jönsson, A.-S. & Wallberg, O. 2009. Cost estimates of kraft lignin recovery by ultrafiltration. *Desalination,* 237**,** 254-267.

Jönsson, B. 2003. Poisson-Boltzmann equation (PB-cell) in the electroneutral cell. Lund, Sweden: Lund University.

Kringstad, K. P. & Roland, M. 1983. ^{13}C-NMR spectra of kraft lignins. *Holzforschung,* 37**,** 237-244.

Labidi, J., Tejado, A., Pena, C., Angulo, V. & Jimenez, L. Isolation and characterisation of lignins from different black liquors. 5th international conference on non-wood fiber pulping an papermaking, 8-10 November 2006 Guangzhou, China. 320-324.

Lake, M. A. & Blackburn, J. C. 2011. *Process for recovering lignin.* USA patent 13/147.785.

Landucci, L. L. 1985. Quantitative ^{13}C NMR characterization of lignin 1. A methodology for high precision. *Holzforschung,* 39**,** 355-360.

Landucci, L. L., Ralph, S. A. & Hammel, K. E. 1998. ^{13}C NMR characterization of guaiacyl, guaiacyl/syringyl and syringyl dehydrogenation polymers. *Holzforschung,* 52**,** 160.

Larsson, S. & Miksche, G. E. 1971. Gaschromatographische analyse von ligninoxydationsprodukten. IV zur struktur des lignins der birke. *Acta Chemica Scandinavia,* 25**,** 647-662.

Lawoko, M., Berggren, R., Berthold, F., Henriksson, G. & Gellerstedt, G. 2004. Changes in the lignin-carbohydrate complex in softwood kraft pulp during kraft and oxygen delignification. *Holzforschung,* 58**,** 603.

Lawoko, M., Henriksson, G. & Gellerstedt, G. 2005. Structural differences between the lignin−carbohydrate complexes present in wood and in chemical pulps. *Biomacromolecules,* 6**,** 3467-3473.

Lee, R., Stack, K., Richardson, D., Lewis, T. & Garnier, G. 2012. Effect of shear, temperature and pH on the dynamics of salt induced coagulation of wood resin colloids. *Colloids and Surfaces A: Physicochemical and Engineering Aspects,* 396**,** 106-114.

Li, S. & Lundquist, K. 1994. A new method for the analysis of phenolic groups in lignins by ^{1}H NMR spectroscopy. *Nordic Pulp and Paper Research Journal,* 9**,** 191-195.

Lin, S. Y. 1992. Commercial spent pulping liquors. *In:* Lin, S. & Dence, C. (eds.) *Methods in Lignin Chemistry.* Berlin, Germany: Springer-Verlaug.

Lin, S. Y. & Detroit, W. Chemical heterogeneity of technical lignins - its significance in lignin utilization. The 1st international symposium on wood and pulping chemistry, 1981 Stockholm, Sweden. 44-52.

Lindström, T. 1979. The colloidal behaviour of kraft lignin. Part I. Association and gelation of kraft lignin in aqueous solutions. *Colloid and Polymer Science,* 257**,** 277-285.

Lindström, T. & Westman, L. 1980. The colloidal behaviour of kraft lignin. Part III. Swelling behaviour and mechanical properties of kraft lignin gels. *Colloid and Polymer Science,* 258**,** 390-397.

Lundquist, K. 1991. ^{1}H NMR spectral studies of lignins Quantitative estimates of some types of structural elements. *Nordic Pulp and Paper Research Journal,* 6**,** 140-146.

Lundquist, K. 1992a. ^{1}H NMR spectral studies of lignins. Results regarding the occurrence of beta-5 structures, beta-beta structures, non-cyclic benzyl aryl ethers, carbonyl groups and phenolic groups. *Nordic Pulp and Paper Research Journal,* 6**,** 4-816.

Lundquist, K. 1992b. Proton (^{1}H) NMR Spectroscopy. *In:* Lin, S. Y. & Dence, C. W. (eds.) *Methods in Lignin Chemistry.* Berlin, Germany: Springer-Verlag.

Marton, J. 1964. On the structure of kraft lignin. *Tappi,* 47**,** 713-719.

Marton, J. 1971. Reactions in alkaline pulping *In:* Sarkanen, K. V. & Ludwig, C. H. (eds.) *Lignins: occurrence, formation, structure and reactions.* New York, USA: Wiley-Interscience.

Mcnaughton, J. G., Yean, W. Q. & Goring, D. a. I. 1967. Macromolecular properties of kraft lignins from spruce made soluble by a continuous flow process. *Tappi,* 50**,** 548-553.

Meier, H. 1958. Studies on hemicelluloses from pine (*Pinus silvestris L.*). *Acta Chemica Scandinavia,* 12**,** 1911-1918.

Merewether, J. W. T. 1957. A lignin-carbohydrate complex in wood: a review of the literature. *Holzforschung,* 11**,** 65.

Min, D., Smith, S. W., Chang, H. & Jameel, H. 2013. Influence of isolation condition on structure of milled wood lignin characterized by quantitative ^{13}C nuclear magnetic resonance spectroscopy. *BioResources,* 8**,** 1790-1800.

Mörck, R. & Kringstad, K. P. 1985. ^{13}C-NMR spectra of kraft lignins II. Kraft lignin acetates. *Holzforschung,* 39**,** 109-119.

Mörck, R., Reimann, A. & Kringstad, K. P. 1988. Fractionation of kraft lignin by successive extraction with organic solvents. III. Fractionation of kraft lignin from birch. *Holzforschung,* 42**,** 111-116.

Mörck, R., Yoshida, H., Kringstad, K. P. & Hatakeyama, H. 1986. Fractionation of kraft lignin by successive extraction with organic solvents. I. Functional groups, ^{13}C NMR spectra and molecular weight distributions. *Holzforschung,* 40**,** 51-56.

Musha Y, G. D. 1974. Klason and acid-soluble lignin content of hardwoods. *Wood Science* 7**,** 133-134.

Nagy, M., Kosa, M., Theliander, H. & Ragauskas, A. J. 2010. Characterization of CO_2 precipitated kraft lignin to promote its utilization. *Green Chemistry,* 12**,** 31-34.

Niemelä, K. & Alén, R. 1999. Characterization of pulping liquors. *In:* Sjöström, E. & Alén, R. (eds.) *Analytical methods in wood chemistry, pulping, and papermaking.* Heidelberg, Germany: Springer-Verlaug

Norgren, M. 2001. On the physical chemistry of kraft lignin: fundamental and applications. Ph.D thesis, Lund University. Lund, Sweden.

Norgren, M., Edlund, H. & Wågberg, L. 2002. Aggregation of lignin derivatives under alkaline conditions. Kinetics and aggregate structure. *Langmuir,* 18**,** 2859-2865.

Norgren, M., Edlund, H., Wågberg, L., Lindström, B. & Annergren, G. 2001. Aggregation of kraft lignin derivatives under conditions relevant to the process. Part I. Phase behaviour. *Colloids and Surfaces A: Physicochemical and Engineering Aspects,* 194**,** 85-96.

Norgren, M. & Lindström, B. 2000a. Dissociation of phenolic groups in kraft lignin at elevated temperatures. *Holzforschung,* 54**,** 519.

Norgren, M. & Lindström, B. 2000b. Physico-chemical characterization of a fractionated kraft lignin. *Holzforschung,* 54**,** 528-534.

Öhman, F. & Theliander, H. 2006. Washing lignin precipitated from kraft black liquor. *Paperi ja Puu,* 88**,** 287-292.

Öhman, F. & Theliander, H. 2007. Filtration properties of lignin precipitated from kraft black liquor. *Tappi,* 6**,** 3-9.

Öhman, F., Wallmo, H. & Theliander, H. 2007a. An improved method for washing lignin precipitated from kraft black liquor - the key to a new biofuel. *Filtration,* 7**,** 309-315.

Öhman, F., Wallmo, H. & Theliander, H. 2007b. A novel method for washing lignin precipitated from kraft black liquor - Laboratory trials. *Nordic Pulp and Paper Research Journal,* 22**,** 9-16.

Öhman, F., Wallmo, H. & Theliander, H. 2007c. Precipitation and filtration of lignin from black liquor of different origin. *Nordic Pulp and Paper Research Journal,* 22**,** 188-193.

Pitzer, K. S. 1991. Ion interaction approach: theory and data correlation. *In:* Pitzer, K. S. (ed.) *Activity coefficients in electrolyte solutions.* 2nd Ed. Boca Raton, USA: CRC Press.

Pu, Y. & Ragauskas, A. J. 2005. Structural analysis of acetylated hardwood lignins and their photoyellowing properties. *Canadian Journal of Chemistry,* 83**,** 2132-2139.

Pye, E. K. 2008. Industrial lignin production and applications. *Biorefineries-Industrial Processes and Products.* Wiley-VCH Verlag GmbH.

Ralph, J. & Landucci, L. L. 2010. NMR of lignins. *In:* Heitner, C., Dimmel, D. & Schmidt, J. A. (eds.) *Lignin and Lignans: Advances in Chemistry.* Boca Raton, USA: CRC Press.

Rezanowich, A. & Goring, D. a. I. 1960. Polyelectrolyte expansion of a lignin sulfonate microgel. *Journal of Colloid Science,* 15**,** 452-471.

Robert, D. R., Bardet, M., Gellerstedt, G. & Lindfors, E. L. 1984. Structural changes in lignin during kraft cooking Part III. On the structure of dissolved lignins. *Journal of Wood Chemistry and Technology,* 4**,** 239-263.

Rudatin, S., Sen Yasar, L. & Woerner Douglas, L. 1989. Association of kraft lignin in aqueous solution. *Lignin: Properties and Materials.* American Chemical Society.

Samuel, R., Pu, Y., Raman, B. & Ragauskas, A. 2010. Structural characterization and comparison of switchgrass ball-milled lignin before and after dilute acid pretreatment. *Applied Biochemistry and Biotechnology,* 162**,** 62-74.

Sevastyanova, O., Helander, M., Chowdhury, S., Lange, H., Wedin, H., Zhang, L., Ek, M., Kadla, J. F., Crestini, C. & Lindström, M. E. 2014. Tailoring the molecular and thermo–mechanical properties of kraft lignin by ultrafiltration. *Journal of Applied Polymer Science,* 131**,** 131-141.

Shaw, D. J. 1993. Colloid stability. *In:* Shaw, D. J. (ed.) *Introduction to colloid and surface chemistry.* 4th Ed. Oxford: Elsevier.

Sjöström, E. 1993. *Wood chemistry: fundamentals and applications,* USA, Academic Press.

Skogsindustrierna 2010. The Swedish forest industries – facts and figures 2010.

Skogsindustrierna 2014. The forest industry-facts and figures 2013.

Sudo, K. & Shimizu, K. 1992. A new carbon fiber from lignin. *Journal of Applied Polymer Science,* 44**,** 127-134.

Sundin, J. 2000. Precipitation of kraft lignin under alkaline conditions., Royal Institute of Technology, Stockholm, Sweden. Stockholm, Sweden.

Tanistra, I. & Bodzek, M. 1998. Preparation of high-purity sulphate lignin from spent black liquor using ultrafiltration and diafiltration processes. *Desalination,* 115**,** 111-120.

Tarja Tamminen, T. V., Maija Tenkanen, Tiina Hausalo, Bo Hortling. Analysis of lignin and lignin-carbohydrate complexes isolated from black liquor. The 8th international symposium on wood and pulping chemistry, 1995 Helsinki, Finland. 297-302.

Tenkanen, M., Tamminen, T. & Hortling, B. 1999. Investigation of lignin-carbohydrate complexes in kraft pulps by selective enzymatic treatments. *Applied Microbiology and Biotechnology,* 51**,** 241-248.

Tessie Du Motay, C. M. 1872. *Improvement in recovering waste alkalis used in treating paper-pulp*. USA patent 132452.

The American Forest and Paper Association. 2003. High production volume (HPV) chemical chalolenge program: final data summary for spent pulping liquor. US: US environmental protection agency.

Theander, O. & Westerlund, E. A. 1986. Studies on dietary fiber. 3. Improved procedures for analysis of dietary fiber. *Journal of Agricultural and Food Chemistry,* 34**,** 330-336.

Theliander, H. Withdrawing lignin from black liquor by precipitation, filtration and washing. Nordic Wood Biorefinery Conference, 11-14 March 2008 Stockholm, Sweden. 36-42.

Toledano, A., García, A., Mondragon, I. & Labidi, J. 2010a. Lignin separation and fractionation by ultrafiltration. *Separation and Purification Technology,* 71**,** 38-43.

Toledano, A., Serrano, L., Garcia, A., Mondragon, I. & Labidi, J. 2010b. Comparative study of lignin fractionation by ultrafiltration and selective precipitation. *Chemical Engineering Journal,* 157**,** 93-99.

Tomani, P. 2010. The LignoBoost process. *Cellulose Chemistry and Technology,* 44**,** 53-58.

Uloth, V. C. & Wearing, J. T. 1989a. Kraft lignin recovery: acid precipitation versus ultrafiltration. Part I. Laboratory test results. *Pulp and Paper Canada,* 90**,** 67-71.

Uloth, V. C. & Wearing, J. T. 1989b. Kraft lignin recovery: acid precipitation versus ultrafiltration. Part II. Technology and economics. *Pulp and Paper Canada,* 90**,** 34-37.

Vainio, U., Maximova, N., Hortling, B., Laine, J., Stenius, P., Simola, L. K., Gravitis, J. & Serimaa, R. 2004. Morphology of dry lignins and size and shape of dissolved kraft lignin particles by X-ray scattering. *Langmuir,* 20**,** 9736-9744.

Valmet. 2013. *Future Valmet to supply a LignoBoost plant for the new biorefinery at the Stora Enso Sunila mill in Finland* [Online]. Metso Corporation's press. Available: http://www.valmet.com/en/infocenter/news.nsf/NewsItems/1747009?OpenDocument.

Velez, J. & Thies, M. C. 2013. Solvated liquid-lignin fractions from a kraft black liquor. *Bioresource technology,* 148**,** 586-590.

Villar, J., Caperos, A. & Garcia-Ochoa, F. 1996. Precipitation of kraft black liquors by alcohol-calcium solutions. *Separation science and technology,* 31**,** 1721-1739.

Wada, S., Iwamida, T., Iizima, R. & Yabe, K. 1962. The bonds between thiolignin and synthetic rubber. VII. Fractional precipitation of thiolignin from kraft pulping waste liquor with the variation of pH and reinforcement of SBR with each fraction. *Kobunshi Kagaku (The chemistry of high polymers),* 19**,** 699-703.

Wallberg, O., Jönsson, A.-S. & Wimmerstedt, R. 2003. Fractionation and concentration of kraft black liquor lignin with ultrafiltration. *Desalination,* 154**,** 187-199.

Wallmo, H., Richards, T. & Theliander, H. 2009a. An investigation of process parameters during lignin precipitation from kraft black liquors: A step towards an optimised precipitation operation. *Nordic Pulp and Paper Research Journal* 24**,** 158-164.

Wallmo, H., Theliander, H., Jönsson, A.-S., Wallberg, O. & Lindgren, K. 2009b. The influence of hemicelluloses during the precipitation of lignin in kraft black liquor. *Nordic Pulp and Paper Research Journal,* 24**,** 165-171.

Wallmo, H., Theliander, H. & Richards, T. 2007. Lignin precipitation from kraft black liquors: kinetics and carbon dioxide absorption. *Paperi ja Puu,* 89**,** 436-442.

Wallmo, H., Wimby, M. & Anders, L. 2009c. Increase production in your recovery boiler with LignoBoost-Extract valuable lignin for biorefinery production and replacement of fossil fuels. *TAPPI Engineering, Pulping, Environmental Conference* Memphis, Tennessee.

Watanabe, T. 2003. Analysis of native bonds between lignin and carbohydrate by specific chemical reactions. *In:* Timell, T. E. (ed.) *Association between lignin and carbohydrates in wood and other plant tissues.* Berlin, Germany: Springer-Verlag.

Wells Jr, T., Kosa, M. & Ragauskas, A. J. 2013. Polymerization of kraft lignin via ultrasonication for high-molecular-weight applications. *Ultrasonics Sonochemistry,* 20**,** 1463-1469.

Whitfield, M. 1975. Electroanalytical chemistry of sea water. *In:* Riley, J. P. & Skirrow, G. (eds.) *Chemical oceanography.* 2nd Ed. New York, USA: Academic Press.

Wigell, A., Brelid, H. & Theliander, H. 2007. Degradation/dissolution of softwood hemicellulose during alkaline cooking at different temperatures and alkali concentrations. *Nordic Pulp and Paper Research Journal***,** 488-494.

Yasuda, S., Fukushima, K. & Kakehi, A. 2001. Formation and chemical structures of acid-soluble lignin Part I. Sulfuric acid treatment time and acid-soluble lignin content of hardwood. *Journal of wood science,* 47**,** 69-72.

Zavitsas, A. A. 1967. Acid ionization constants of phenol and some hydroxy-methylphenols between 20 degree and 60 degree. *Journal of Chemical & Engineering Data,* 12**,** 94-97.

APPENDIX I

Calculation of the degree of dissociation of the phenolic groups on a lignin molecule (α) using the PB cell programme

In the calculation, the weight-average molecular weight of the kraft softwood lignin is 11.8 kDa (DMSO/10 mM LiBr GPC, UV detector) and its density ($\rho_{lig.}$) is 1349.5 kg m^{-3} (Norgren and Lindström, 2000a). By assuming that the lignin molecule is a rigid sphere, its radius ($R_{lig.}$) can be calculated by:

$$R_{lig.} = \left(\frac{3}{4\pi}V_{lig.}\right)^{\frac{1}{3}} = \left(\frac{3}{4\pi}\frac{Mw_{lig.}}{N_A\rho_{lig.}}\right)^{\frac{1}{3}} \tag{A}$$

where $V_{lig.}$ (m^3) is the volume of the lignin molecule and N$_A$ is Avogrado's constant (6.022E 10^{23}).

R_{cell} is calculated by:

$$R_{cell} = \left(\frac{3}{4\pi}V_{cell}\right)^{\frac{1}{3}} = \left(\frac{3}{4\pi}\frac{Mw_{lig.}}{N_A\rho_{BL}[L-O^-]_{BL}}\right)^{\frac{1}{3}} \tag{B}$$

where V_{cell} (m^3) is the volume of the lignin molecule and ρ_{BL} (kg m^{-3}) is the density of the black liquor calculated by the method proposed by Clay (2011). [L–O$^-$]$_{BL}$ is the concentration of lignin ([L–OH$_{aq.}$] + [L–O$^-$]) in the filtrate, which is obtained from Klason lignin experimental data. The input of cations in the programme, *i.e.* the concentration of (Na$^+$ +K$^+$) and hydrogen ions, is also provided by experimental data, and {H$^+_{bulk}$} is known at a given pH measurement value. In order to calculate the value of {H$^+_{surf.}$} at the surface of the lignin molecules, the concentration of hydrogen ions in the bulk has to be estimated from both the activity and the activity coefficient, followed by a calculation of the surface concentration using the PB cell programme. The surface concentration allows the activity of the H$^+$ to be estimated. However, since the activity coefficients are assumed to be approximately constant in the cell, and the concentration of protons has no significant effect on the electrostatic potential (due to the extremely low concentration), a simplification of the calculation procedure is made by exchanging the concentration of the protons in the bulk directly with the measured activity; the activity at the surface is simulated directly using the PB cell programme.

Examples of the calculation of α using a PB cell programme are shown in Table C.

The differences in the calculated values of {H$^+_{surf.}$} between using {H$^+_{bulk}$} and divalent ions in the PB cell programme were also evaluated; the deviation was found to be less than 0.38%.

Table C. Examples of data used in a PB cell programme and the calculated values of α from softwood BL.

pOH		4.44	3.9	3.42	2.92	3.03	3.09
T	°C	45	45	45	75	65	45
$[\text{L–O}^-]_{\text{BL}}$	g kg^{-1} liq.	17.1	21.7	36.1	71.5	66.6	60.7
ρ_{BL}	Kg m^{-3}	1170	1180	1180	1160	1170	1180
$R_{\text{lig.}}$	Å	15.1	15.1	15.1	15.1	15.1	15.1
R_{cell}		61.5	56.8	47.9	38.3	39.2	40.3
σ^{-1}	Å^2 charge^{-1}	-4710	-1745	-938	-872	-863	-724
$[\text{Na}^++\text{K}^+]$	mM L^{-1}	3350	3380	3380	3340	3350	3380
$\{\text{H}\}^+_{\text{bulk}}$		1.10E-06	3.18E-07	1.05E-07	1.67E-07	1.33E-07	4.93E-08
$\{\text{H}\}^+_{\text{surf.}}$		1.11E-06	3.21E-07	1.07E-07	1.70E-07	1.35E-07	5.03E-08
α		0.113	0.306	0.569	0.612	0.619	0.738

APPENDIX II

Carbohydrate Analysis

The contents of cellulose, (galacto)glucomannan and xylan were calculated using carbohydrate analysis, with the following assumptions/corrections being made:

The amounts of sugars analyzed were corrected for the acid hydrolysis yield. Anhydro sugars were calculated from sugar monomers by the withdrawal of water (multiplied by 0.88 and 0.90 in the case of pentosans and hexosans, respectively). Glucomannan was calculated as the sum of the galactan, mannan and part of the glucan. The molar ratio between the mannose and the glucose in the galactoglucomannan was assumed to be 3.5:1 (Meier, 1958). All of the galactan measured was included in the (galacto)glucomannan. Acetyl groups were, however, not included. Xylan was calculated as the sum of both the xylan and arabinan: all of the arabinan measured was included in the xylan. Cellulose was calculated as the content of glucan after withdrawal for the contribution of glucan to (galacto)glucomannan.

(Galacto)glucomannan = Galactose + [1+ (1/3.5)] × Mannose

Xylan = Xylose + Arabinose

Cellulose = Glucose − (1/3.5) × Mannose

The analyses were summarized in a mass balance based on the assumption that the carbohydrates were divided into cellulose, (galacto)glucomannan and xylan, which were calculated as described above.